

RESEARCH

Open Access



# Properties of Concrete and Structural Behaviour of Reinforced Concrete Beam Containing Shredded Waste Paper as An Additive

B. A. Solahuddin\* and F. M. Yahaya

## Abstract

This research uses WP to investigate the effect of two types of Shredded Waste Paper (SWP) comprising Shredded Copier Waste Paper (SCPWP) and Shredded Cardboard Waste Paper (SCBWP) as additives on the properties of concrete and the structural behaviour of Reinforced Concrete Beam (RCB). The slump, compressive, flexural, and splitting tensile strengths increase by 4–13% for 5–10% addition of SCPWP and decrease by 16–23% for 15% addition of SCPWP compared to 0% addition. For SCBWP, the slump, compressive, flexural and splitting tensile strengths increase by 10–23% for 5–10% addition and decrease by 15–21% for 15% addition compared to 0% addition. 15% of SCPWP and SCBWP addition records the highest effect in water absorption and efflorescence, showing 11% and 10.28% increases with 15% addition of SCBWP and SCPWP. Scanning electron microscope (SEM) analysis reveals that the crack is repaired, and the presence of calcium hydroxide (Ca(OH)<sub>2</sub>) and calcium–silicate–hydrate (C–S–H) links enhances the concrete strength. The addition of 10% SCPWP and 10% SCBWP in the concrete mixtures improves the structural behaviour of RCB with stirrup spacing (SS) = 100 mm (full), 150 mm and 200 mm (reduced) by increasing the load and reducing the deflection. Apart from that, the concrete bending and shear strains also increase by 44.17% and 34.9%. The failure mode of the RCB changes from shear to bending. This study indicates that SCPWP and SCBWP can be used as additives in concrete at 5% and 10%, and 10% for RCB with significant strength and structural improvement.

**Keywords** Shredded waste paper, Concrete, Reinforced concrete beam, Mechanical properties, Durability properties, Structural behaviour

## 1 Introduction

If we wish to untie economic growth from ecological degradation, we must improve our resource efficiency. There is a finite amount of Earth's resources, and their extraction causes adverse effects on the environment and

the climate. That is why resource efficiency is crucial for a greener, more circular economy in the world, as well as for long-term production and consumption habits. Water, sand, cement, and coarse aggregate are the fundamental materials used for concrete making. Paper cement pulp is created when cement and waste paper (WP) are combined with water. Once the pulp has dried, it can be a durable building material. A concrete mixture containing WP is excellent for insulating and long shelf life because of its sturdy nature. In a range of construction sizes, it is a structurally and economically viable alternative, as demonstrated through experimental results (Titzman, 2006). The use of WP reduces the quantity of cement needed as

Journal information: ISSN 1976-0485 / eISSN 2234-1315

\*Correspondence:

B. A. Solahuddin

[solahuddin.08@yahoo.com](mailto:solahuddin.08@yahoo.com)

Faculty of Civil Engineering Technology, Universiti Malaysia Pahang,  
Lebuhraya Tun Razak, 26300, Gambang, Kuantan, Pahang Darul Makmur,  
Malaysia



© The Author(s) 2023. **Open Access** This article is licensed under a Creative Commons Attribution 4.0 International License, which permits use, sharing, adaptation, distribution and reproduction in any medium or format, as long as you give appropriate credit to the original author(s) and the source, provide a link to the Creative Commons licence, and indicate if changes were made. The images or other third party material in this article are included in the article's Creative Commons licence, unless indicated otherwise in a credit line to the material. If material is not included in the article's Creative Commons licence and your intended use is not permitted by statutory regulation or exceeds the permitted use, you will need to obtain permission directly from the copyright holder. To view a copy of this licence, visit <http://creativecommons.org/licenses/by/4.0/>.

the main building material in construction, which also makes it more environmentally friendly (Yun et al., 2011).

The fundamental constituent is the WP, which originate from various sources, such as ordinary paper, cardboard, magazine, garbage mail, publicising brochures, or any other types of used paper. Most of the published works on WP recycling are from the paper mill (Bai et al., 2003; Chin, et al., 1998; Chun et al., 2007; Gallardo & Adajar, 2006; Kraus, et al. (2003; Naik et al., 2004) or manufactured cement board (Fuwape et al., 2007; Okino et al., 2000). WP embodies a vital source of cellulose, fibre, and conjointly foremost types of waste found in all activity areas. Researchers use waste paper in concrete and reinforced concrete beam (RCB) mixtures to decrease and avoid dumping waste in landfills. Furthermore, according to Thiswaran and Varma (2017), WP can be utilised correctly by reducing the density of the construction material. The inclusion of WP in concrete is being studied to reduce construction costs by evaluating its quality, workability, and other attributes (Titzman, 2006). Its lightweight properties make it suitable for internal walls in seismically active high-rise buildings. The reinforced concrete's dead load and the number of steel necessary can also be reduced, resulting in considerable savings in labour and energy costs (Thiswaran, 2018). Moreover, it saves landfill space and prevents chemicals used in paper processing and dispensing out of the groundwater (Malthy & Jegatheeswaran, 2011).

Hospodarova et al., (2018) showed that composites made with cellulosic fibres had a 6.8% lower density and a 34% lower thermal conductivity than the reference sample. Hardened fibre cement specimens with plasticiser had greater dispersion of cement particles and enhanced bond strength between fibres and matrix, resulting in the highest values of compressive (48.4 MPa) and flexural (up to 7 MPa) strengths. The preliminary findings from the experimental tests indicated that if the volumetric ratios of solid waste paper and paper pulp were increased by 2%, 5%, and 10%, the flexural and compressive strengths of the specimens decreased (Cardinale et al., 2021). As the percentage of solid waste paper rose, its ability to absorb water increased. However, the opposite trend was seen in the case of paper pulp usage. This proved that papercrete could be used as a novel eco-friendly construction material, with well-suited physical and mechanical features for structurally reinforcing existing masonry panels (Cardinale et al., 2021).

The concrete compressive strength values increased by 17%, 30%, and 46%, followed by flexural strength by 77%, 272%, and 795%, respectively, when 1%, 2%, and 3% wire steel fibres were added to reference sample (Özkılıç et al., 2022). Compressive strength increased by 11.2%, 21.7%, and 32.5%, respectively, when concrete

was mixed with 1%, 2%, and 3% waste lathe scraps compared to the concrete mixture without no waste materials (Karalar et al., 2022a). Fibre-reinforced concrete's compressive and splitting tensile strengths were improved when lathe scrap was added to the mix. Still, the concrete became less workable above a certain amount of steel fibre content (Çelik et al., 2022a). Increasing waste lathe content in fibre-reinforced concrete boosted the concrete's flexural strength. 20% WGP substitution with cement appeared to be the optimum percentage (Zeybek et al., 2022). The combined waste glass significantly improved the strength and produced better workability, suggesting that 10% replacement level was the optimum. Bottom ash was used as a replacement for fine aggregate in concrete, with typical substitution ratios at 25%, 50%, 75%, and 100% (Karalar et al., 2022b). The optimal displacement capacity was achieved at 75% bottom ash ratio (BAR)s. The beam's ability to bend was diminished as the BAR increased to 100%. The second problem with BAR was that 75% strain caused the reinforced concrete structure to severely displace. Qaidi et al. (2022) use recycled waste glass (WG) to replace fine aggregate in self-compacting concrete mixtures at volumes ranging from 10 to 50%. The slump was improved by 2%, 5%, 8%, 11%, and 85% after including 10%, 20%, 30%, 40%, and 50% of WG.

The flexural strengths rose by 3.2%, 6.3%, 11.1%, and 4.8% when fine aggregate and coarse aggregate were replaced with waste glass at 10%, 20%, 40%, and 50%, respectively (Çelik et al., 2022b). 20% waste glass replacement was the optimum. Shear cracks were first observed, but flexural cracks were observed as the proportion of waste marble powder in the concrete mixture increased from 0 to 40% (Karalar et al., 2022c). Thus, when the longitudinal reinforcement ratio was close to the balanced ratio, 10%–20% of marble waste could be used as cement replacement, and above 20% should be avoided. The volume of coarse aggregate was swapped out with rubber tree seed shells ranging from 2 to 16% (Beskopylny, et al., 2022). The axial compressive and tensile strengths in twisting increased by 6% and 8%, respectively, when coarse aggregate was replaced with 4% rubber tree seed shell by volume. Under axial compression, the strain value decreased by 6%, whereas under axial tension, it decreased by 5%. This result led to a 7% rise in the modulus of elasticity. Reinforcement using coconut fibres was varied from 0% to 2.5%, increasing by 0.25 wt.% at each range (Shcherban et al., 2022). The optimal amount of coconut fibre was found to be 1.75%. Both compression and axial compression mechanical indicators rose by 24%, while tensile bending and axial tension mechanical indicators rose by 42% and 43%, respectively. The maximum stress increased by 46% in compression and 51% in

tension. The elastic modulus was also affected, showing a 16% increase.

The paper–cement matrix consisted of 12% cement, 10% of coconut shell powder, and 0, 0.5, 1.0, 1.5, 2.0, and 2.5 wt.% of palm kernel fibre (Akinwande et al., 2021a). The obtained results demonstrated that the sample properties were improved with increasing fibre content. The total property ratio for each mixture showed that the alkaline-treated fibre (TPKF) performed better than the untreated fibre (UPKF). Waste paper pulp, unmodified banana fibres (UMBF) and modified banana fibres (AMBF), fine sand, and ordinary portland cement (OPC) were mixed into paper bricks (Akinwande et al., 2021b). Different amounts of fibre by waste paper pulp weight were added by 0%, 0.5%, 1%, 1.5%, 2%, and 2.5% and cured for 28 and 56 days, respectively. The water absorption increased with fibre percentages, although the samples reinforced with AMBF absorbed less water volume than those reinforced with UMBF. Increasing the fibre percentage content increased the samples' compressive, flexural, and splitting tensile strengths. In order to create the control mix, a combination of 10% cement (by clay volume) and 20% sand (by clay volume) was made (Akinwande et al., 2022). The waste wig fibre (WWF) was added to other mixtures in varying percentages, from 1 to 5% by clay volume. WWF considerably helped enhance hydro-resisting qualities by lowering porosity levels, water and moisture absorption, capillary suction, and water permeability. The results suggested that WWF could reinforce cement adobe bricks at an optimal mix of 5% volume percentage by increasing the water and moisture susceptibility resistance followed by improving the mass and dimensional stability.

This research is conducted to determine the potential of SCPWP and SCBWP as additives in concrete and RCB. It could be seen that WP was less used in concrete and never been used in any of structural application. Moreover, the WP type's significance has not been studied and highlighted yet in any research before this. Hence, this research studies the effect of two types of SWP comprising SCPWP and SCBWP on concrete properties by investigating the workability, compressive, flexural and splitting tensile strengths, water absorption, and efflorescence. Moreover, this research also studies the structural behaviour by investigating the load–deflection, load–strain, ultimate load-bearing capacity, and failure mode of shredded waste paper reinforced concrete beam (SWPRCB) upon the inclusion of the best percentage of SCPWP and SCBWP as additives. On a greater scale, the use of SWP in concrete production is a potential alternative to minimise paper wastage and reduce solid waste pollution. Besides that, the government have reiterated their aspiration towards implementing green technology

and combating global warming. The innovation of new materials is expected to offer extra revenue and contribute to improving the construction technology. Paper is made from wood. Wood comes from a tree. If the usage of paper is uncontrolled, more trees will be cut, and this will cause more logging and deforestation to occur. Under these circumstances, it is hopeful that the development of concrete through the incorporation of SWP would reduce logging and deforestation.

## 2 Materials and Methods

### 2.1 Materials

The Orang Kuat brand is a type of Ordinary Portland Cement (OPC) manufactured by YTL Cement Marketing Sdn. Bhd. This cement was used throughout this study as it fulfils the Type 1 Portland cement of Malaysian Standard MS 522: Part 1 (2003) properties, as shown in Table 1.

River sand supplied by a local supplier was used as the fine aggregate. The properties of the river sand fulfilled the requirements of BS 882 (1992), with the values of specific gravity, fineness modulus, and water absorption of the sand being 2.68, 2.72, and 0.82, respectively. Physically, the sand particles are angular and well graded. The cumulative passing weight for river sand is 98.94%. Based on the result, the fine aggregate sieve analysis result is located between the minimum and maximum cumulative percentage passing, which follows the guideline of the BS 812: Part 103 (1985) standard and is located in zone IV (80%–100%). Therefore, it is suitable to be used as a fine aggregate. Granite was chosen as the raw material for this study because it is a good material for coarse aggregate. The granite was obtained from a local supplier following BS 882 (1992) standards. The cumulative passing weight for granite is 100%. The result was well within the percentage pass, where the coarse aggregate sieve analysis result was located between the minimum and

**Table 1** OPC properties (MS522, 2003)

Test	Units	Test result	MS 522-1: 2007 (42.5N)
Physical properties			
Soundness	mm	1.00	≤ 10
Fineness	m <sup>2</sup> /kg	345	–
Initial setting time	min	130	≥ 60
Chemical properties			
Sulphate content (SO <sub>4</sub> <sup>2-</sup> )	%	2.70	≤ 3.5
Loss on ignition (LoI)	%	3.20	≤ 5.0
Chloride (Cl <sup>-</sup> )	%	0.02	≤ 0.1
Insoluble residue	%	0.40	≤ 5.0

maximum cumulative percentage passing based on the BS 812: Part 103 (1985) standard and is located in zone IV (80–100%). This study used tap water. 6.5–8.5 is the neutral pH of tap water, and it is compatible to be used in the concrete mixing process. The amount of water used in this study was 0.5 based on the W/C ratio. The water used must be clean and impurities free to avoid influencing the specimen result. As an outcome, the water utilised for producing and curing ought to be sensibly perfect and liberated from harmful materials, like acid, oil, alkali, salt, and other elements which might be detrimental to the concrete. The copier and cardboard waste paper samples were collected from the office. Fig. 1a, b shows the SCPWP and SCBWP used.

A paper shredder machine was used to shred the CPWP and CBWP to obtain SCPWP and SCBWP with a uniform size. The size of SCPWP after shredded is 1.2 cm × 0.2 cm × 0.01 cm (length (*l*) × width (*w*) × thickness (*t*)), while for SCPWP, the size after shredded is 1.2 cm × 0.2 cm × 0.05 cm (length (*l*) × width (*w*) × thickness (*t*)), as shown in Table 2. It can be seen that only the thickness has different values, while the length and width values are the same. SCBWP has a higher thickness than SCPWP. All SCPWP and SCBWP will be completely disintegrated when mixing in a concrete mixture. Before disintegration, the SWP is not shredded. After disintegration, the SWP is shredded to a smaller size using a paper shredder machine. The test's purpose for the disintegration properties is to determine and compare the fibre properties of SCPWP and SCBWP before and after disintegration and whether any differences or improvements could be observed. Table 2 shows the fibre properties of SCPWP and SCBWP before and after disintegration. Based on the tables, it can be seen that SCBWP has higher average fibre lengths as well as fibre content compared to SCPWP for both before and after disintegration. The

**Table 2** SWP fibre properties (Borysiuk et al., 2017)

SWP types	Average fibre length (mm)		Fibre content (%)	
	Before disintegration (mm)	After disintegration (mm)	Before disintegration (%)	After disintegration (%)
SCPWP	1.23	1.33	18	28
SCBWP	1.27	1.37	22	32

fibre properties increase and become better after disintegration compared to before disintegration (Borysiuk et al., 2017).

Microfibrils of cellulose have a degree of elasticity until they are broken. The chiral angle of the microfibrillar helix determines cellulose's elastic modulus of 25 GPa (Prasad et al., 2015), and the modulus of elasticity can be calculated by applying a strain parallel to the fibre axis. Compared to other angles, the angle of microfibrils is more likely to fluctuate naturally, bringing its average value closer to the fibre axis. This means the fibre has an elastic modulus similar to cellulose. The tiny asymmetry image shows the twist and chirally curl of SWP fibres, as depicted in Fig. 2.

SWP is predominantly made of wood cellulose, a fibrous material that provides structural strength. Cellulose is composed of long sugar-like molecules, known as β-D glucose, that bind together smaller sugar molecules (Prasad et al., 2015; Zaki et al., 2018). Fig. 3 delineates the cellulose fibre containing polar hydroxide (OH) groups that form hydrogen bonds and bunch up cellulose chains. The chains pack together and form stable, hard crystalline regions, which provide more outstanding balance and support. This hydrogen bonding positively impacts the concrete strength by raising its strength (ASTM C, 1609).

This research utilised three types of rebars, which were selected based on the manual calculation design



(a) Shredded copier waste paper (SCPWP) (b) Shredded cardboard waste paper (SCBWP)

**Fig. 1** Shredded waste paper (SWP)

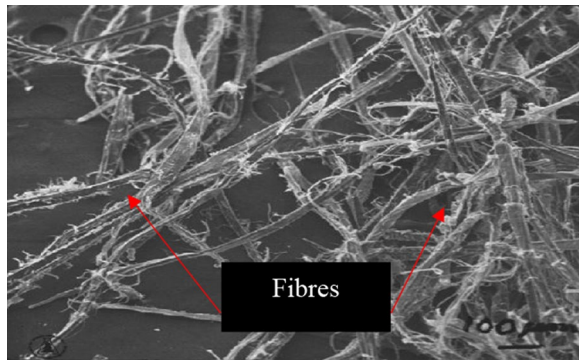


**Fig. 2** SWP fibres (Prasad et al., 2015)

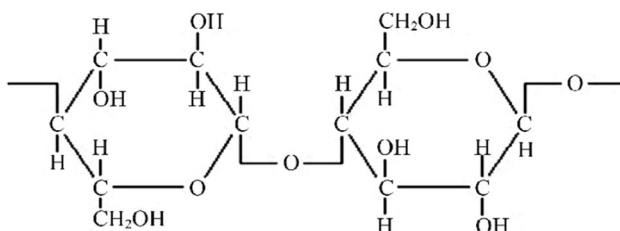


**Fig. 3** Cellulose hydrogen bond (Prasad et al., 2015; Zaki et al., 2018)

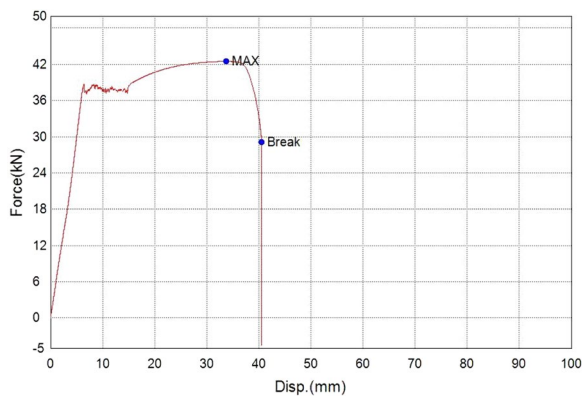


**Fig. 4** Tensile test graph for H6, H12, and H16 rebars

following the (ASTM C, 1609). The first and second rebars were the high yield steel of 460 N/mm<sup>2</sup> and 500 N/mm<sup>2</sup> grade (namely, the 2H12 and 2H16), while the third was the mild steel of 250 N/mm<sup>2</sup> grade (namely, H6). The 2H16 was used for tension reinforcement, while 2H12 was used for compression reinforcement. Meanwhile, H6 was used for the stirrup spacing (SS), which is also called the shear link, with a size of 100 mm, 150 mm, and 200 mm. Fig. 4 shows the tensile test graph for H6, H12, and H16 rebars.

## 2.2 Mix Proportion of Concrete

In this study, seven mixes were prepared, which consisted of one control mix and six proposed mixes. The control mix specimen consists of 0% addition of SCPWP and SCBWP, while the proposed mix specimens comprised 5%, 10%, and 15% additions of SCPWP and SCBWP, respectively. The control specimen containing 0% SWP was prepared as ordinary concrete to compare the performance of other concrete with SWP. The ratio used for Grade 30 concrete was 1:0.75:1.5 (cement:sand:aggregate) based on (Emmanuel Ofori, 2019; Civil E Blog, 2020; Construction Cost, 2021). The W/C ratio used was 0.5, as recommended by Uniform Building Code, (2017), which is the optimum value given that the concrete surface was in a closed place, placed in water, and not exposed to sunlight. The amount of SWP used was based on the total weight of each specimen. For example, the total weight for the SCPWP1 mixture is 196 kg. Hence, a 5% addition of SWP in the SCPWP1 mixture equals to 9.8 kg (5% × 196 kg = 9.8 kg). Table 3 shows the Grade 30 proportion.

Meanwhile, typical reinforced concrete making processes were used for the RCB preparation. A concrete mixer was used to mix all the materials after they were rightly weighed based on the mix design. To ensure an identical mix proportion, SCPWP and SCBWP were added to the concrete with 5%, 10%, and 15% by weight of the mixture, respectively, for all specimens except the

**Table 3** Grade 30 proportion

Concrete mixture sample	Cement (kg/m <sup>3</sup> )	Sand (kg/m <sup>3</sup> )	Aggregate (kg/m <sup>3</sup> )	SWP		W/C ratio
				(%)	(kg/m <sup>3</sup> )	
C	50	37.5	75	0	0	0.5
SCPWP1	50	37.5	75	5	9.38	0.5
SCPWP2	50	37.5	75	10	18.75	0.5
SCPWP3	50	37.5	75	15	28.13	0.5
SCBWP1	50	37.5	75	5	9.38	0.5
SCBWP2	50	37.5	75	10	18.75	0.5
SCBWP3	50	37.5	75	15	28.13	0.5

**Table 4** Grade 30 proportion for RCB

Concrete mixture	Cement (kg/m <sup>3</sup> )	Sand (kg/m <sup>3</sup> )	Aggregate (kg/m <sup>3</sup> )	SWP		W/C ratio
				(%)	(kg/m <sup>3</sup> )	
0% C	75	56.25	112.5	0	0	0.5
10% SCPWP	75	56.25	112.5	10	28.13	0.5
10% SCBWP	75	56.25	112.5	10	28.13	0.5

control (0% SWP). Table 4 presents three concrete mix proportions utilised.

### 2.3 Preparation Process of Shredded Waste Paper Concrete

In order to produce the concrete, several steps of preparation were conducted. Initially, all the mixing ingredients, such as water, coarse aggregate, cement, sand, and SWP, were precisely weighed to the required amount. Prior to the mixing, the collected SWP waste was shredded using

a shredder paper machine. All the materials were then mixed using a cleaned and debris-free concrete mixer until an equivalent mix was acquired as shown in Fig. 5a. Then, the concrete mixing was carried out by utilising a rotating drum type mixer with 56 kg capacity, which complied with the BS 1881: Part 125 (2013) standard. In order to guarantee uniformly mixed concrete, the ensuing step was executed. The coarse aggregate was first added into the concrete mixer prior to the fine aggregate,



(a) Mixing concrete materials in a concrete mixer



(b) Concrete compaction using a vibration table



(c) Each concrete cube and concrete beams were marked



(d) Water curing

**Fig. 5** Preparation process of shredded waste paper concrete

cement, and SWP. The components were mixed well for the first 2 min. Accordingly, 75% of the mixing water was added to the dry mix and mixed for an additional 2 min, where the remaining water was added gradually into the mix. The compaction of the concrete was done based on the BS 1881: Part 108 (1983) standard. Upon completing the mixing process, the mix was taken out, filled into the mould and placed on the vibrating table for the compaction process, as depicted in Fig. 5b. A wet gunny sack was used to cover the mould after the compaction and afterwards kept overnight before demoulded. Finally, all specimens were marked and subjected, as delineated in Fig. 5c. All the specimens were cured with water curing. The water absorption test was used as the durability testing in this research. All the specimens were demoulded after 24 h and placed in the chosen curing regime until the necessary age of testing. Fig. 5d shows that the concrete cube and concrete beam specimens were submerged in the potable water bath tank.  $24 \pm 5$  °C was the potable water bath temperature and it was in the range of

room temperature. This is an ideal temperature for concrete mixing.

#### 2.4 Main Reinforcement Details of Reinforced Concrete Beam

The control SWPRCB (0% SWP addition), 10% SCPWP, and 10% SCBWP beams consist of three SS. All beams have a rectangular cross-section with the same size of 150 mm, 200 mm, 1500 mm ( $w \times h \times l$ ), and a span of 400 mm. The details of the beam and reinforcement are illustrated in Figs. 6 and 7. The concrete cover ( $C_{nom} = 30$  mm) is used for all beams. Since concrete is intended for real practical applications, it is necessary to ensure that the test beam dimensions are sufficiently large to simulate a real structure element. The beam size and length are also chosen to ensure that the beam will fail in shear (shear span to an effective ratio of more than 4.0). Sufficient shear links of H6-100, H6-150, and H6-200 mm are provided outside the 400 mm loading zone to avoid flexural failure.

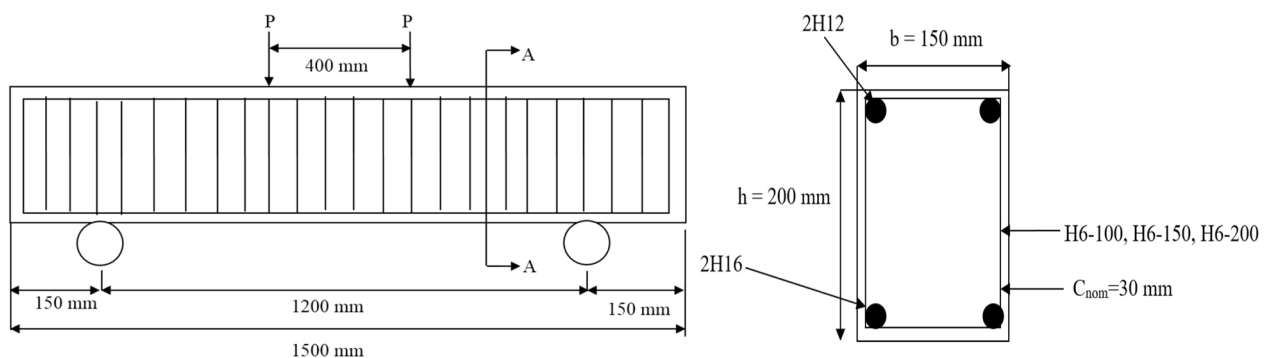


**Fig. 6** Reinforced concrete beam details



**Fig. 7** Reinforced concrete beam reinforcement

## 2.5 Preparation Process of Shredded Waste Paper Reinforced Concrete Beam

The 2H16 and 2H12 bars were placed at the bottom and top of the RCB. H6-100, H6-150, and H6-200 indicate three different types of stirrup spacing. The concrete was mixed using a drum mixer and poured into a 0.045 m<sup>3</sup> mould. At first, all the dry ingredients were put together, followed by water to achieve the desired mixture consistency and good concrete workability. The SCPWP and SCBWP were added at the end before adding more water



**Fig. 8** Casted reinforced concrete beam

and the mixing time was increased from 5 to 10 min. The formwork was then entirely filled with the concrete mixture and a table type vibrator was used to achieve full compaction. Lastly, all the RCB were air cured for 28 days prior to testing (Fig. 8).

## 3 Results and Discussion

### 3.1 Concrete

This section presents the result of the fresh property, known as slump, of the concrete specimens. Next, the mechanical properties results, including the compressive strength, flexural strength, and splitting tensile strength, were based on the 7 and 28 days of water curing concrete specimen. Finally, the durability properties explain the water absorption and efflorescence test results.

#### 3.1.1 Slump

From Fig. 9 the slump value increased by 3.85% and 6.73% with 5% SCPWP and SCBWP, respectively. The slump value further increases by 5.56% and 6.31% with 10% SCPWP and SCBWP. At 15% addition, the slump value drops by 19.3% and 18.64%. Overall, it can be seen from Fig. 10 that the slump value of concrete containing SCBWP is higher than that of SCPWP. The study found by Gallardo and Adajar (2006) that 5% to 10% waste paper (WP) addition was the most suitable mix proportion to replace the fine aggregate and further addition over 10% decreased the workability and reduced the slump value. The slump increased up to 5% cement replacement with WP, while the slump value decreased as the WP content in the concrete mixture increased above 5% (Balwaik

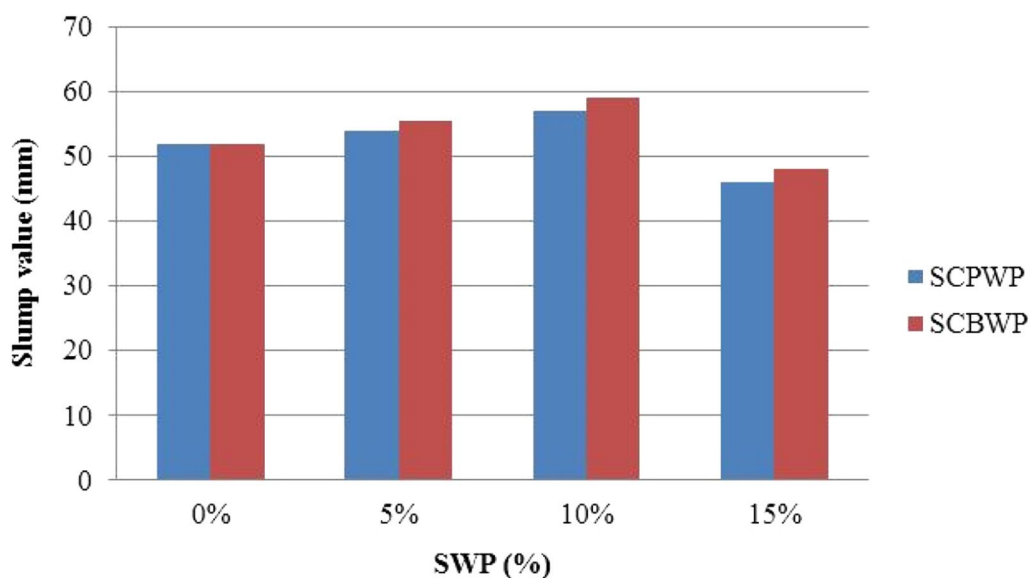


**Fig. 9** Slump

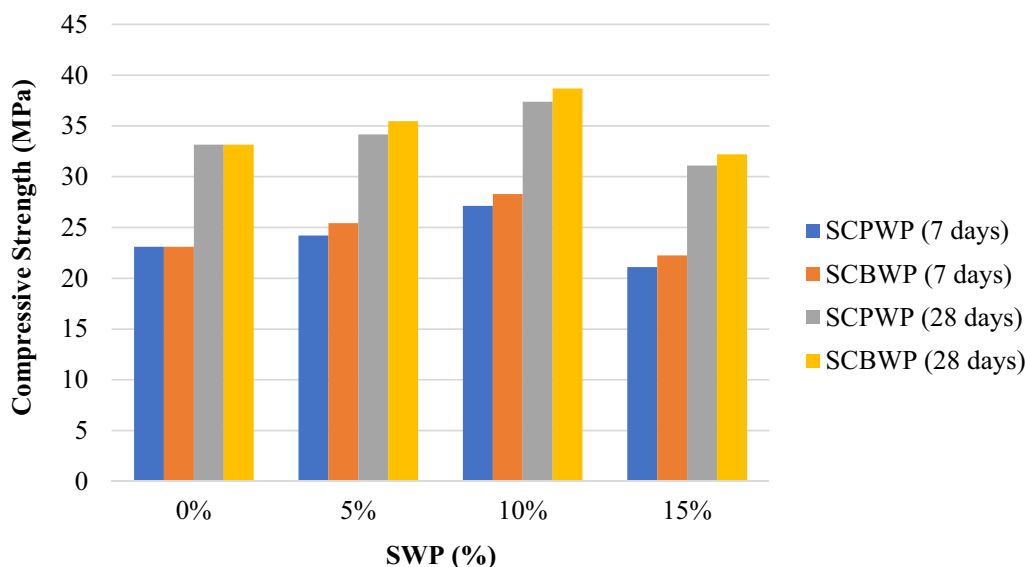


**Fig. 10** Compressive strengths (7 and 28 days)

& Raut, 2011). The concrete mixture required more water to achieve the desired slump value when a higher amount of SWP was added. This is due to the decreasing density of concrete with higher SWP content. On the contrary, the concrete workability improves by adding a high amount of water rather than admixtures to attain an economically feasible concrete. In view of this, the workability of concrete containing residual SWP is achieved by adding excessive water rather than admixtures to produce economic concrete. Nevertheless, several variables could lead to antagonistic impacts on the workability and density of concrete, such as the amount of SWP addition, the physical properties of SWP, and the carbon content of SWP (Zaki et al., 2018).

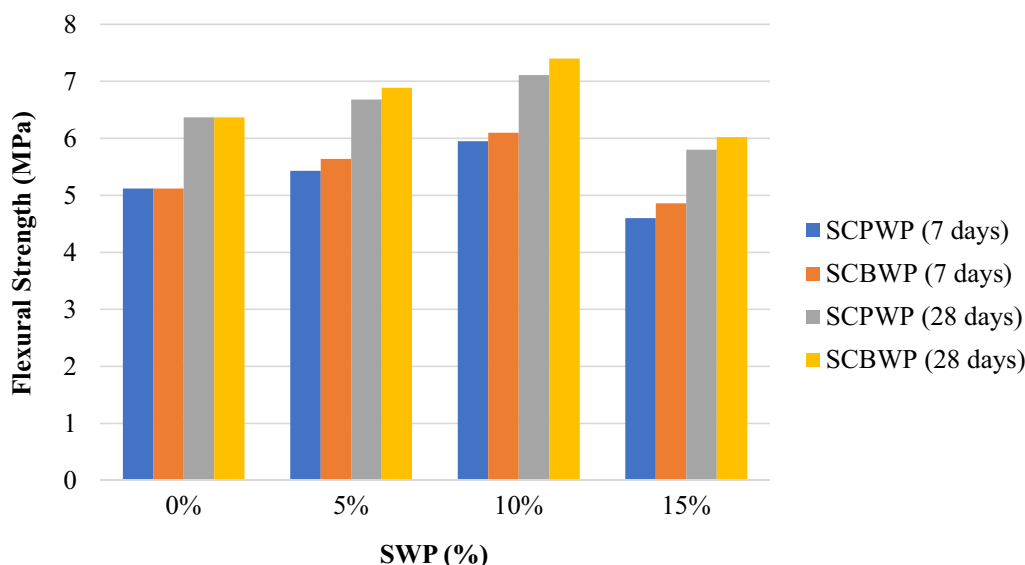
### 3.1.2 Compressive Strength

Fig. 10 shows the compressive strength test results from the water curing of concrete at the age of 7 and 28 days. At 7 days, the compressive strengths increase by 4.8% at 5% and 12.06% at 10% but decrease by 22.25% at 15% addition of SCPWP. Meanwhile, for concrete with SCBWP, the compressive strengths increase by 10.04% at 5% and 11.29% at 10% but decrease by 21.38% with 15% addition. At 28 days, the compressive strength values increase by 3.05% and 7% with a 5% addition of SCPWP and SCBWP, respectively. The strength value also increases with 10% addition by 9.42% and 9.08%, respectively. At 15% additions of SCPWP and SCBWP, the compressive strength values fall by 16.82% and 16.77%. In short, the 10% addition of both SWP produces the optimum compressive strength at 7 and 28 days with water curing since the value starts decreasing at 15% addition

for both types of SWP. The study concluded by Balwaik and Raut (2011) that the best mix proportion consisted of 5–10% replacement of WP with cement. The compressive strength typically increased up to 10% WP, which subsequently decreased as WP was increased. An increase of 10% and 15% in the compressive strength was observed with 5% WP at 7 and 28 days, respectively, before the strength gradually decreased (Malik, 2013). The highest compressive strength measured was 15% more than the reference mix (0% WP) at 28 days. The result indicates that the strength is affected by various factors, such as the SWP addition percentage and the types of SWP used. The percentage of each SWP addition undergoing the curing age at 7 days are visualised through the compressive strength bar chart in Fig. 28. The test results show an increment of compressive strength as the curing age is prolonged due to the hydration process in the concrete mixture. At 7 and 28 days test ages, the compressive strength of the concrete mixtures with 5% and 10% additions SCPWP and SCBWP is higher than that of the control mixture since the mixtures with SWP contain a significant amount of alumina-siliceous material that reacts with calcium that improves the compressive strength of the concrete (Zaki et al., 2018).

### 3.1.3 Flexural Strength

The impact of the SWP addition on the flexural strengths of concrete is shown in Fig. 11, which illustrates the average 7 and 28 days flexural strengths of the concrete specimen, respectively. The addition of 5% and 10% of SCPWP and SCBWP achieves an increase of 16.21% and 19.14% of flexural strengths compared to



**Fig. 11** Flexural strengths (7 and 28 days)

the control and other concrete mixtures at 7 days. However, the flexural strengths with 15% of SCPWP and SCBWP drastically decrease below the control mix's strength by 22.69% and 20.33%, respectively. At 28 days, the average flexural strengths of the concrete specimen with 5% addition of SCPWP and SCBWP increase by 4.87% and 8.16%, while for 10% addition, the flexural strengths increase by 6.44% and 7.4%, respectively. However, the flexural strengths for the concrete mixtures with 15% of SCPWP and SCBWP decrease rapidly below the strength of the control mixture by 18.42% and 18.65%, respectively. Although the flexural strength decreases using 15% addition for both SWP, the flexural strength of concrete containing SCBWP is still higher than that of SCPWP. Based on the results by Ghani and Mohammad Shukeri (2008), 5% and 10% mixtures containing WP showed higher strength than 0% mixture. However, the concrete's flexural strength declined as the WP content more than 10%. The findings indicate that 5% to 10% was the suitable percentage of WP as a partial Portland cement replacement (Balwaik & Raut, 2011). The flexural strength increased until 10% of WP in the mixture before the flexural strength gradually reduced above 10%. The concrete fails due to the flexure test. The strength of concrete is substantially reduced with a reduction in cohesion. The results indicate that all mixtures yielded comparable or higher flexural strength (modulus of rupture) than the curing ageing control mixture. Therefore, it can be assumed that most of the concrete specimens show no detrimental effects (i.e. strength reversal) when using SCPWP and SCBWP over an extended curing period.

### 3.1.4 Splitting Tensile Strength

Fig. 12 shows the results of splitting tensile strength of the cylindrical concrete specimens subjected to water curing at 7 and 28 days of curing ageing. At 7 days, the splitting tensile strengths increase by 5.69% and 15.01% at 5% and 10% addition of SCPWP, respectively, but decrease by 26.6% at 15% addition. Meanwhile, the splitting tensile strengths of 5%, 10% and 15% addition of SCBWP increase by 15.27% and 10.91% at 5% and 10%, respectively, but decrease by 25.29% at 15% addition. At 28 days, the splitting tensile strength values increase by 7.54% and 12.65% with a 5% addition of SCPWP and SCBWP, respectively. Furthermore, the strength values increase by 9.5% and 11.23% with the inclusion of SCPWP and SCBWP at 10%, respectively. With a tremendous SWP amount of over 10%, the concrete gradually shows a decrease in splitting tensile strength by 22.31% and 22.91%, respectively, with SCPWP and SCBWP addition at the percentage of 15%. Given that the splitting tensile strength increases up to 10% addition of SCPWP and SCBWP before beginning to decrease at 15% addition, therefore, the best percentage of SWP for SCPWP and SCBWP is 10% to produce the highest splitting tensile strength at both days with water curing. The 5% WP mixture showed the highest tensile strength compared to other mixtures (Ghani & Mohammad Shukeri, 2008). At 7 days, the tensile strength of the concrete mix containing WP was roughly 6.1% stronger than the control mix, but the tensile strength reduced to 5.8% at 28 days. Briefly, the splitting tensile strength increased with up to 10% addition of WP and a further increase in WP reduced the strength gradually (Balwaik & Raut, 2011).

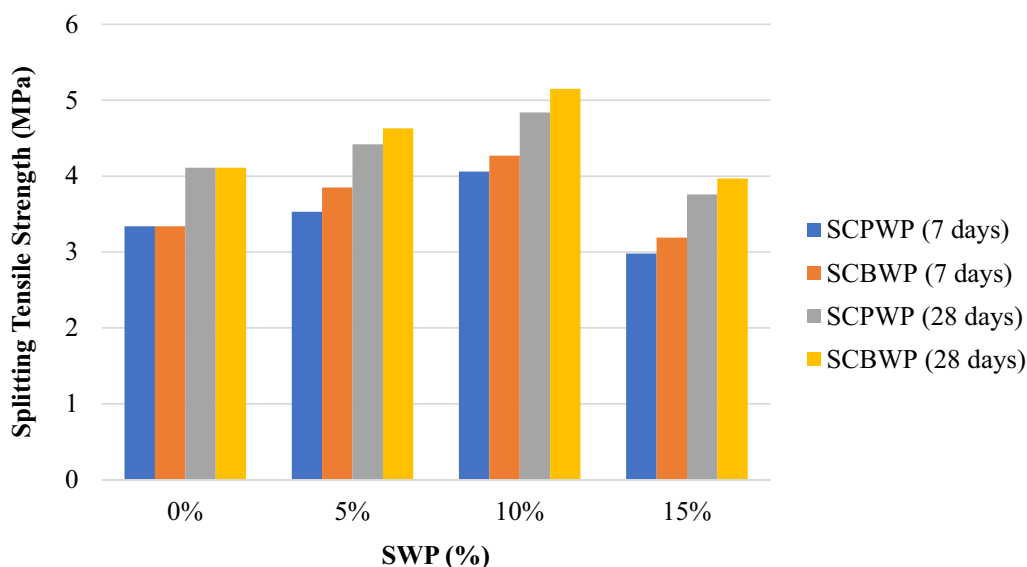


**Fig. 12** Splitting tensile strengths (7 and 28 days)

These findings indicate that the splitting tensile strength is affected by numerous factors, such as the percentage of SWP addition and the type of SWP used. The splitting tensile strength line graph illustrates each percentage of SWP that has undergone curing at 7 and 28 days. All specimens exhibit a strength increment as the curing ageing is prolonged.

### 3.1.5 Discussion

All strengths are much better at 5% and 10% SWP addition than at 0% SWP addition. Cellulose makes up the bulk of SWP. It is a compound of carbon and hydrogen used to make organic fibres. The hydrogen bonds are strengthened when water is added to SWP because oxygen atoms from the water molecules interact with the hydrogen atoms from the cellulose molecules (Zaki et al., 2018). WP also has a high alumina-silica concentration, which reacts favourably with calcium to increase its strength. The alkali drives hydraulic and pozzolanic reactions of the SWP, and, to a lesser extent, the hydration process discharges calcium hydroxide ( $\text{Ca}(\text{OH})_2$ ), which is also substantially associated with the increasing strength. In addition to this, adding 5% and 10% SWP causes the surface of the SWP to be obscured by the hydration products, which decreases the matrix's minor void and porosity. According to Wagih et al. (2013), debonding between the SWP and matrix with lower calcium carbonate ( $\text{CaCO}_3$ ) contents occur during carbonate composite transmigration. When added to a concrete mixture, SWP helps create a dense matrix that boosts its mechanical strength.

The optimal compressive, flexural, and splitting tensile strengths were achieved by incorporating 10% SCPWP and SCBWP. After analysing the microstructure of the concrete specimens with varying SWP levels, Kalapad et al. (2019) concluded that the physical properties of SWP were responsible for the strength increase with 10% addition. Because the fine aggregate in concrete binds the matrix together, it has greater compressibility than regular concrete and can alleviate the stretch concentration. As a result of the SWP particle's high fibre content, the concrete matrix becomes more cohesive, improving the material's mechanical properties. Scanning electron microscope (SEM) images by Prasad et al. (2015), Borysiuk et al. (2017), and Zaki et al. (2018) show that the interfacial progress zone distinguishes the strong bonding of particles with the cement paste. On the contrary, this study found that more than 10% SWP addition was ineffective in improving the concrete properties. An excessive amount of SWP will keep and retain specimens' volume, and any development will reduce the concrete materials bond. Thus, the concrete strength will become weak. The increased porosity of the concrete from the excessive addition of SCPWP and SCBWP caused a decrease in the concrete strength. The loss of strength was due to the weak cohesion as well as the acutely poor binding of cellulosic material in the calcium-silicate-hydrate (C-S-H) gel (Zaki et al., 2018). The reduction of the strength was also strongly related to the amount of SWP addition, physical properties, and carbon content. Furthermore, the increment of SCPWP and SCBWP percentages resulted in low silica content in the composition. Besides, a higher addition of SWP causes a thicker

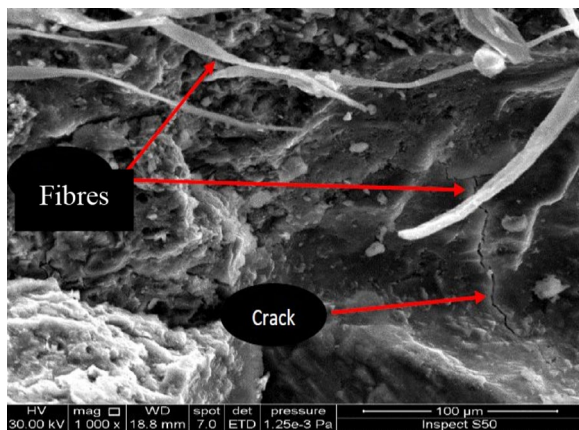


**Fig. 13** 0% SWP

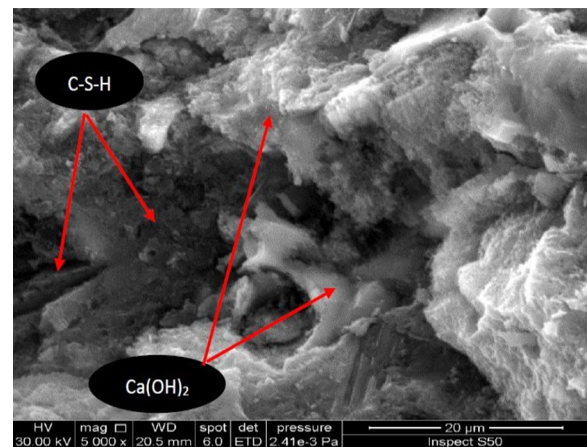


**Fig. 14** 5% SWP

surface texture and the formation of inner voids and capillary channels that negatively impacts the cohesion and quality of the concrete.

Previous investigations had similar results. According to research by Jung et al. (2015), increasing the amount of SWP used to replace cement paste reduced the binding strength between the two materials. The micrograph results of another investigation showed that microcracks formed from the bond zone due to poor bonding properties between SWP (10% addition) and cement paste (Kalapad et al., 2019). Increasing the SWP % in the concrete mixture correlated with the specimen's closed pores (Sangrutsamee et al., 2012). Overall, the tensile, flexural, and compressive strengths drop after the SCPWP and SCBWP contents reach 15% and above. Additionally, at 7 and 28 days, SCBWP has greater compressive, flexural, and splitting tensile strengths than SCPWP with a 5%, 10%, or 15% addition. When compared to SCPWP, SCBWP is denser, heavier, and has a greater proportion of medium and long fibre contents in its fibres (Borysiuk et al., 2017). Since SCBWP contains more cellulose than SCPWP, it was hypothesised that more hydrogen bonds would be formed between the oxygen atoms in water and the hydrogen atoms in cellulose, leading to greater compressive, flexural, and splitting tensile strengths. Compared to SCPWP, SCBWP would be more rigid, robust, vigorous, and long lasting.

### 3.2 Scanning Electron Microscope of Concrete Containing Shredded Waste Paper

The SEM or microscopic structures of 0%, 5%, 10%, and 15% SWP addition are shown in Figs. 13, 14, 15, 16. The cement paste is well bonded with particles when observed using a SEM. SWP hydration products are clearly visible on the SWP surface, as shown in Figs. 13 and 14. The experimental results show that the pores

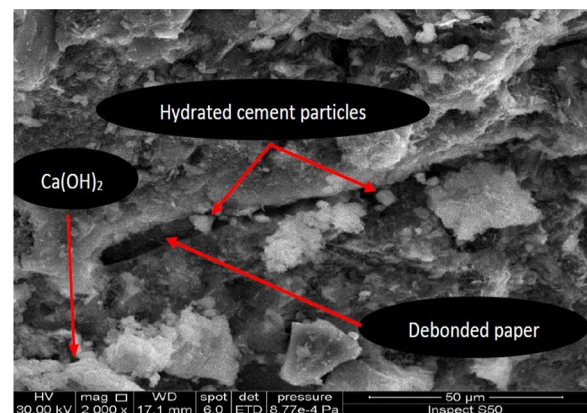


**Fig. 15** 10% SWP

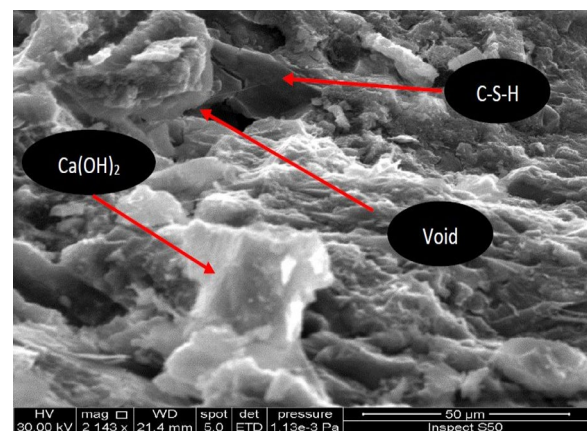


**Fig. 16** 15% SWP

in the matrix have been reduced and fewer voids have been found in the matrix. As a result, SWP additive enhances the concrete properties. Figs. 15 and 16 show

the debonding between SWP and cement paste with a moderate proportion of calcium carbonate ( $\text{CaCO}_3$ ) by considering the transmigration of carbonate composites. Insufficient bond zone between SWP and cement paste causes microcracks to occur, as shown by the results, which observed from the SEM images. This causes the pores in the concrete to become more tightly bonded. There is a crack in Fig. 13 without SWP contents and fixed at 5% SWP content in Fig. 14. The calcium hydroxide ( $\text{Ca}(\text{OH})_2$ ) compound and calcium-silicate-hydrate (C-S-H) bond fix the crack and cause the concrete strength to increase. In Fig. 15, there are some hydrated cement particles, as observed through the SEM. The hydrated cement particles tend to increase the concrete strength more compared to the strength at 5% SWP addition. The strength decreases at 15% SWP addition because of the void caused by excessive SWP content, as shown in Fig. 16. The void replaces the bond of  $\text{Ca}(\text{OH})_2$  and C-S-H causing the bond to become weaker and looser. This causes the concrete strength to decrease. 5% and 10% are the optimum percentages of SWP addition and more than 10% is unsuitable to be added in a concrete mixture.

### 3.2.1 Water Absorption

The water absorption of concrete with different percentages of SCPWP and SCBWP are presented in Fig. 17. The curing period was constrained to 28 days, according to the suggestion by Akinwumi and Gbadamosi (2014). The control concrete (0% SWP addition) produces the lowest water absorptions of 6.3%. In comparison, the water absorption results for 5% addition of SCPWP and

SCBWP are 7.24% and 7.95%, while at 10% addition, the water absorptions are 8.46% for SCPWP and 9.17% for SCBWP, respectively. The highest water absorption is recorded at 11% and 10.28% with 15% addition of SCBWP and SCPWP, respectively. Balwaik and Raut (2011) analysed the water absorption test on the M-20 and M-30 concrete mixtures with WP addition. The concrete water absorption increased with WP content. However, the excessive water content would reduce the concrete strength. Meanwhile, Ghani and Mohammad Shukeri (2008) reported that the higher the WP content led to higher water absorption of concrete. The water absorption rates were 13.9–62.3% and 10.8–118.4% at 7 and 28 days, respectively, compared to the control mixture. The findings indicate that higher utilisation of SWP will increase the water absorption of concrete. The high water absorption might be due to the high porosity of concrete preserved in the air.

Basically, adhesion is the attraction of one kind of molecule to other molecules of a different kind, and it can be very intense for water (Academy, 2016). Water tends to stick to itself in certain conditions but is known to be drawn to other forms of molecules as well. Micropores in the paper chemical structure consist of tiny plant fibre webs. Zaki et al. (2018) discovered that cellulose makes up extended chains of connected sugar molecules. These sugar molecules have unique characteristics which quickly absorb water and retain them for a long time. Cellulose fibres in paper have plenty of empty spaces that appear like tiny bubbles of air between them, which gives paper its absorptive properties. When paper is mixed with water, the water tends to be absorbed and stick to

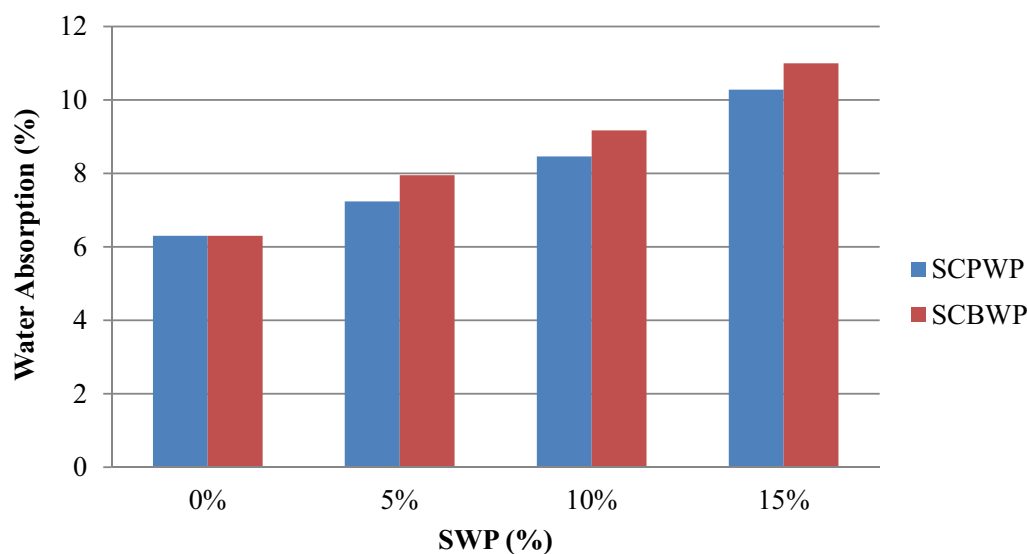


**Fig. 17** Water absorption (28 days)

the paper celluloses. Besides the high water absorption properties of paper, the fibres contain empty spaces, which influence the paper absorbency on the water. The water molecules confine the gaps by interacting with one another as they are attracted by fibre celluloses (Budies, 2015). Thus, more spaces allow more water to be absorbed. The results show that all specimens containing SCPWP and SCBWP have a percentage of less than 10%, so they are deemed high-quality concrete except for 15% SCPWP and SCBWP. High-quality concrete has a water absorption percentage of less than 10% (Neville, 2011).

### 3.2.2 Efflorescence

An efflorescence test aims to identify the common names for the deposits of soluble salts that form in or near the surface of a porous material due to the water's evaporation that was initially dissolved. Nil, slight, moderate, heavy, and serious efflorescence are the five states that can be used to identify a concrete's efflorescence. The cured age of 28 days was used for this evaluation. The efflorescence test data for each percentage replacement type is shown in Figs. 18, 19, and 20. There is no efflorescence deposit on the 0% (control concrete), which is nil (Fig. 18). 5% and 10% addition of SCPWP and SCBWP have a very slight layer of salt deposited (Fig. 19). This efflorescence occurs because SWP properties are made from pulp and contain fibre properties. In contrast, the condition of 15% addition of SCPWP and SCBWP is moderate, covering up to 50% of the exposed concrete surface (Fig. 20). These efflorescence test findings were proven by Balwaik & Raut, (2011) and Malik (2013). They stated that the higher the fibre contents from the waste paper, the higher the salt deposits on the concrete surface.



Nil - When there is no noticeable deposit of efflorescence.

**Fig. 18** 0% SCPWP, 0% SCBWP



Slight - When thin deposit of salts is covered over exposed area of the concrete is less than 10%.

**Fig. 19** 5%, 10% SCPWP; 5%, 10% SCBWP

### 3.3 Reinforced Concrete Beam

This section presents the load–deflection behaviour, load–strain behaviour and ultimate load-bearing capacity of SWPRCB results at 28 days of air curing for the 0% SWPRCB (control) and 10% SWPRCB mixtures. The control RCB mixture without any SWP is designated as 0% C, while the 10% SWPRCB consists of two RCB types, which contain 10% of SCPWP and SCBWP in the mixtures, respectively. The 10% addition is chosen based on the optimum compressive strength in the concrete mixture from the previous section.

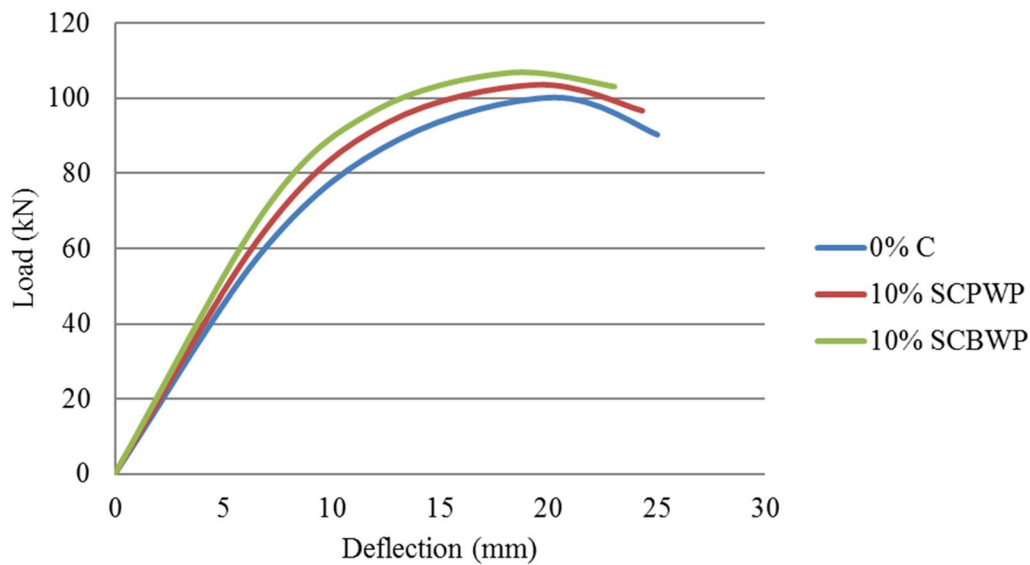
#### 3.3.1 Load–Deflection

Fig. 21 depicts the RCB'S load–deflection curve (SS=100 mm, full shear reinforcement), whereas Figs. 22 and 23 illustrate the RCB's load–deflection curves (SS=150 and 200 mm, reduced shear reinforcements). Tables 5, 6, and 7 outline the key parameters, which include load at yield ( $P_y$ ), yield deflection ( $\delta_y$ ), ultimate load ( $P_u$ ), ultimate deflection ( $\delta_u$ ), maximum load ( $P_{max}$ ) that represents the load-carrying capacity, maximum deflection ( $\delta_{max}$ ), and the ductility ratio ( $\mu$ ),



Moderate - When there is a greater deposit than under slight and covering up to 50% of the exposed area of the concrete surface but unaccompanied by powdering or flaking of the surface.

**Fig. 20** 15% SCPWP, 15% SCBWP



**Fig. 21** Load–deflection (SS = 100 mm)

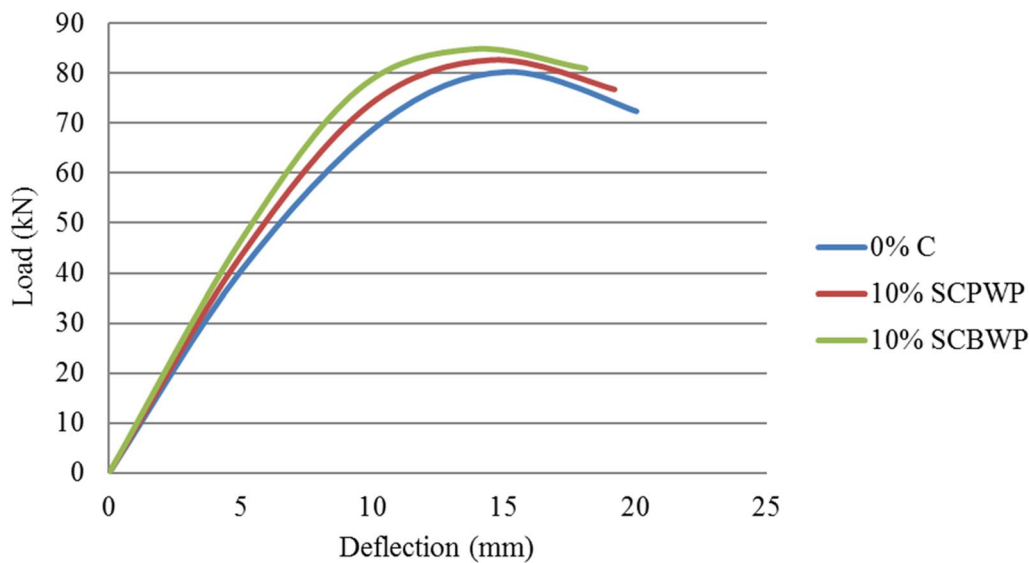


**Fig. 22** Load–deflection (SS = 150 mm)

which is defined as  $\mu = \delta_u / \delta_y$ . The 10% SCPWP and 10% SCBWP RCB test results are significantly different from the 0% C (control RCB) for all types of SS. ASTM-1035 offset method determines the steel yield point. 0.001 is the maximum strain value for the 0% C, assuming that the same stress values have already been yielded by 10% SCPWP and 10% SCBWP RCB.

The addition of 10% SCPWP and 10% SCBWP with 100, 150, and 200 mm of SS, which are the full and reduced shear reinforcements, increases the  $P_y$ ,  $P_u$ , and  $P_{max}$  but decreases the  $\delta_y$ ,  $\delta_u$ , and  $\delta_{max}$  of the RCB. The

RCB with 100 mm of SS containing 10% SCPWP and SCBWP shows various cracking behaviour and pseudo-strain-hardening effect. Although strain hardening is typical behaviour of metal, similar behaviour is often displayed by fibre-reinforced composites accompanied by multiple cracking under increasing load caused by the fibre microcrack arrest, which is proven by experimental work (Li et al., 2013). Nevertheless, the  $P_y$  and  $P_{max}$  improvements for 10% SCPWP and 10% SCBWP RCB with SS = 150 and 200 mm are significant. The  $P_y$  increased because of the increasing dowel movement,

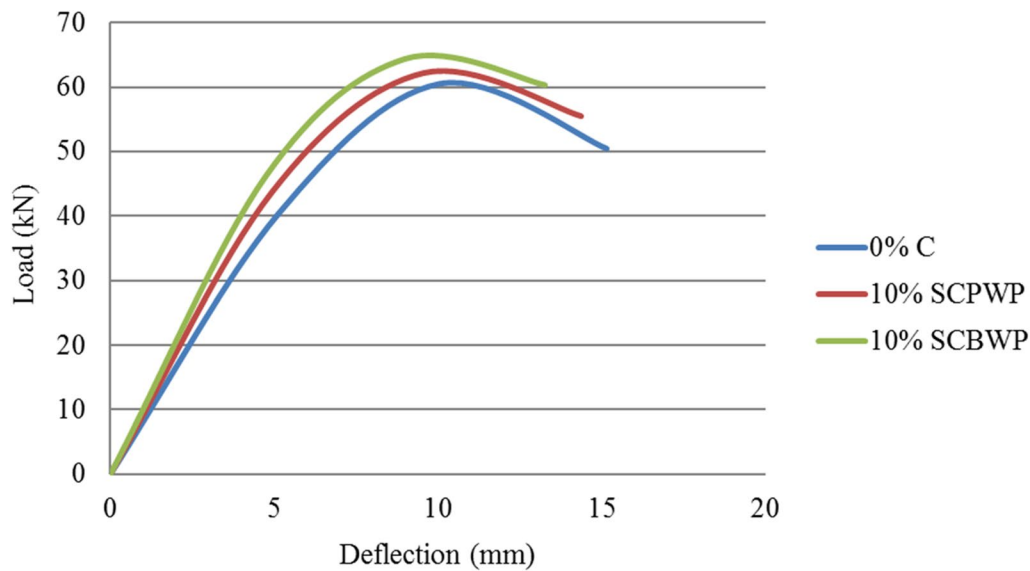


**Fig. 23** Load–deflection ( $SS = 200$  mm)

**Table 5** Load–deflection values ( $SS = 100$  mm)

SWP (%)	$P_y$ (kN)	$\delta_y$ (mm)	$P_u$ (kN)	$\delta_u$ (mm)	$P_{max}$ (kN)	$\delta_{max}$ (mm)	$\mu = \delta_u/\delta_y$
0% C	89.01	13.12	90.23	25.03	100.12	20.27	1.91
10% SCPWP	93.34	12.57	96.56	24.34	103.45	19.45	1.94
10% SCBWP	96.67	11.98	103.15	23.04	106.78	18.12	1.92

**Table 6** Load–deflection values ( $SS = 150$  mm)

SWP (%)	$P_y$ (kN)	$\delta_y$ (mm)	$P_u$ (kN)	$\delta_u$ (mm)	$P_{max}$ (kN)	$\delta_{max}$ (mm)	$\mu = \delta_u/\delta_y$
0% C	70.12	10.36	72.34	20.04	80.23	15.11	1.93
10% SCPWP	73.45	9.87	76.67	19.23	82.56	14.55	1.95
10% SCBWP	76.78	9.46	81.03	18.11	84.89	13.78	1.91

**Table 7** Load–deflection values ( $SS = 200$  mm)

SWP (%)	$P_y$ (kN)	$\delta_y$ (mm)	$P_u$ (kN)	$\delta_u$ (mm)	$P_{max}$ (kN)	$\delta_{max}$ (mm)	$\mu = \delta_u/\delta_y$
0% C	40.36	5.13	50.46	15.16	60.51	10.04	2.96
10% SCPWP	43.58	4.92	55.45	14.38	62.13	9.56	2.92
10% SCBWP	46.27	4.76	60.27	13.27	64.30	8.98	2.79

matrix bond, and aggregate interlock mechanism caused by the fibre from the SWP addition. The  $P_{max}$  value increases after the crack initiated caused by the unique fibre characteristic, which serves as a crack arrestor in the cracking mechanism, as discussed by Martin (2008). Furthermore, the load–deflection curve for the RCB with

10% SCBWP was less deflected than the 0% C and 10% SCPWP.  $SS = 150$  and  $200$  mm proved that the lower the shear reinforcement, the lower the ultimate displacement. Thus, adequate fibre amount in the RCB influenced the increase of  $P_y$ ,  $P_{max}$ , and pseudo-stress-hardening effect (multiple cracking) of the RCB structure.

The  $\mu$  value is obtained by calculating the  $\delta_u$  value concerning the  $\delta_y$  value. In general, a structural member can sustain significant deflection before failure by having a ratio of high ductility. RCB's ductility is essential because the substantial deflection at closing maximum load-bearing capacity should be withstood by each structural member and ample warning should be provided when the structure faulty is near to happen. The RCB's ductility shown by the experimental results increased significantly when a sufficient amount of SWP was added to the concrete mixture. Compared to 0% C, the improvement of maximum ductility is acquired up to 4.68% using RCB with 10% SCBWP at SS=100 mm, while RCB with 10% SCPWP achieves an increase of 5.47% ductility. It is examined that the 10% SCPWP and SCBWP addition in the RCB correlates the ductility improvement up to a certain point before decreasing. Less ductility with stiff and failed RCB occurred due to higher fibre content in the RCB was shown by a similar pattern from Syed Mohsin (2012). The ductility ultimately increases as the crack initiates and the fibre prevents the crack growth and multiple cracks creations. Therefore, the 10% SCPWP and 10% SCBWP inclusion showed an essential improvement in the strength and structure ductility of the RCB as the SCPWP and SCBWP were more brittle than 0% C and able to control the propagation of cracks.

### 3.3.2 Load–Strain

The load–strain results are plotted and analysed to illustrate the bending and shear strain behaviour of 0% C, 10% SCPWP, and 10% SCBWP RCB when the

load was applied. Figs. 24, 25, and 26 show the concrete bending strain in the pure bending region, while Figs. 27, 28, and 29 demonstrate the concrete shear strain encountered in the shear span. In most design codes, the crack width of flexural is the foremost crucial parameter for protecting steel bar from corrosion. However, Khan and Zhang (2000) stated that the shear crack width is not set to any specific limit as the shear crack happens when the foiled structure is assumed to occur. Nevertheless, an ordinary concrete has a maximum strain value of 3000  $\mu\epsilon$ , which can indicate the structure crack width (Sin et al., 2011). As proven in Table 8, 3000  $\mu\epsilon$  is not exceeded for the strain values for all RCB specimens. The results show that RCB with SS=200 mm has higher strain values than SS=150 and 100 mm.

Furthermore, RCB with 10% SCBWP and 10% SCPWP have higher strain values than 0% C for all types of reinforcements. The reducing strain value result is caused by the fibre content from SCPWP and SCBWP. The mechanism of fibre crack bridging prevents the diagonal shear cracking with the presence of fibre through the crack surface by transmitting tensile stress. Besides that, the ultimate strain capacities have been reached by 10% SCPWP and 10% SCBWP RCB under constant service loadings. Hence, from the results, a material consisting of fibre can prevent diagonal tensile cracking. The cracks' width of the RCB can be reduced with fibre inclusion in the concrete mixture. Perhaps, the service load can also be reduced. In conclusion, the fibre content in the SWP hinders the cracks' growth via the crack bridging

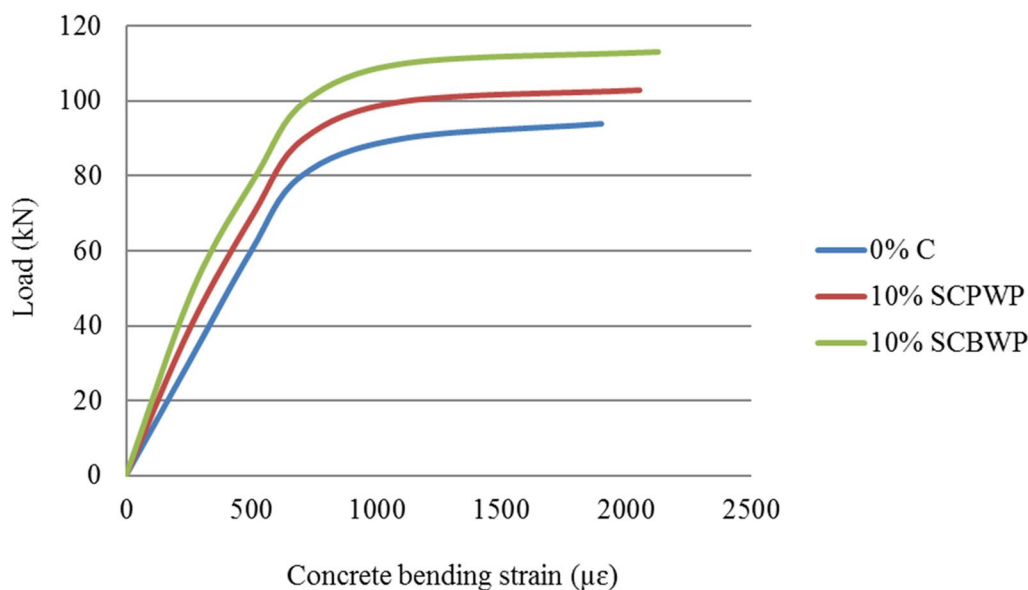


**Fig. 24** Load–strain (SS = 100 mm)

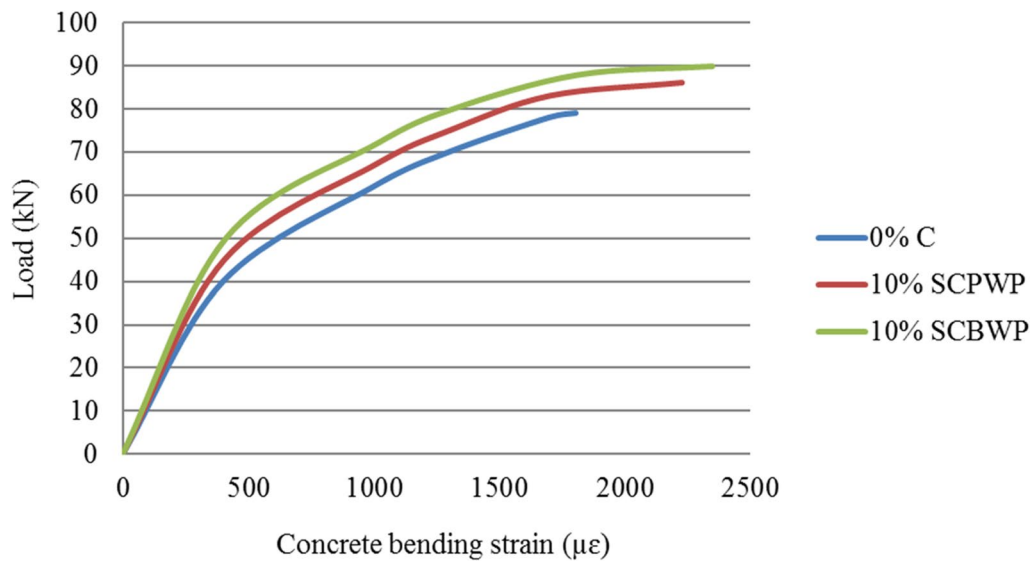


**Fig. 25** Load–strain (SS = 150 mm)

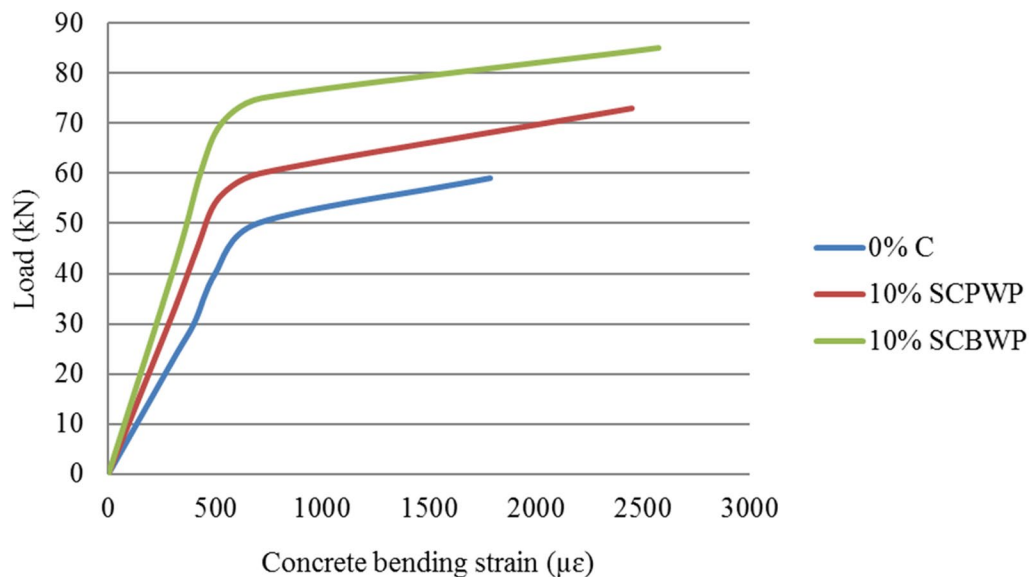


**Fig. 26** Load–strain (SS = 200 mm)

mechanism, which simultaneously lessens the cracks' width and increases the cracks' number.

### 3.3.3 Ultimate Load-Bearing Capacity

The result listed in Table 9 refers to the load at first crack ( $P_1$ ) and ultimate load ( $P_u$ ) of the 0% C (control), 10% SCPWP and 10% SCBWP RCB mixtures with three reinforcements comprising SS=100 mm (full shear reinforcement), 150 and 200 mm (reduced shear reinforcement).

The  $P_1$  of the 0% C takes place at a shear distance of approximately 60.47 kN. Beyond this load, the cracks spread to the top of the RCB and additional flexural cracks were formed along the RCB length. The cracks propagated towards the loading point, forming a straight line and diagonal cracks with further load increase. The load sustainability reaches the highest shear capacity as the extended diagonal cracks reach the loading and support points. An RCB would demonstrate a pseudo-strain-hardening or pseudo-ductility behaviour if many cracks are produced and the  $P_1$  strength is lower than

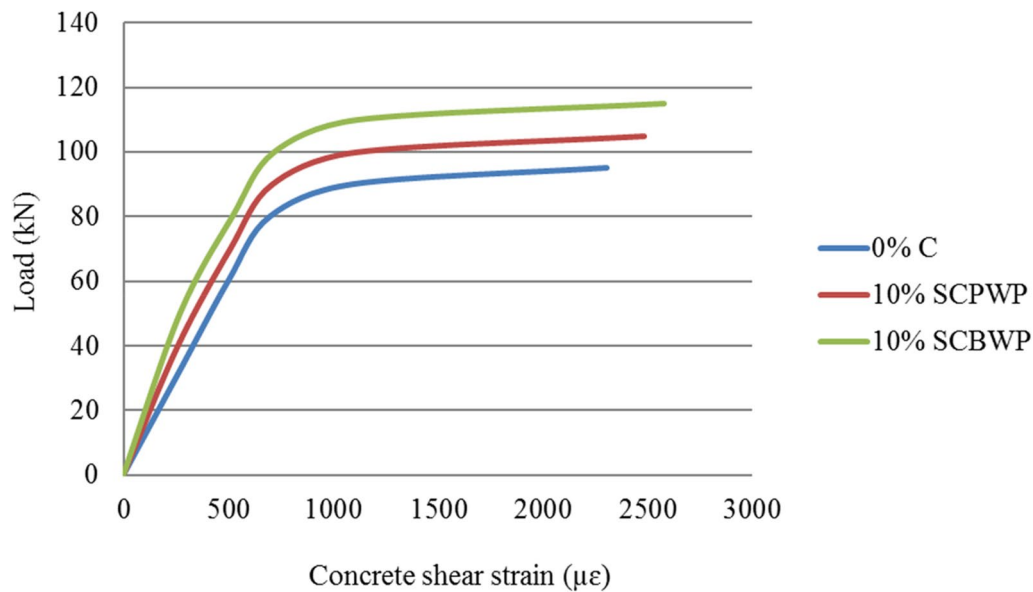


**Fig. 27** Load–strain (SS = 100 mm)

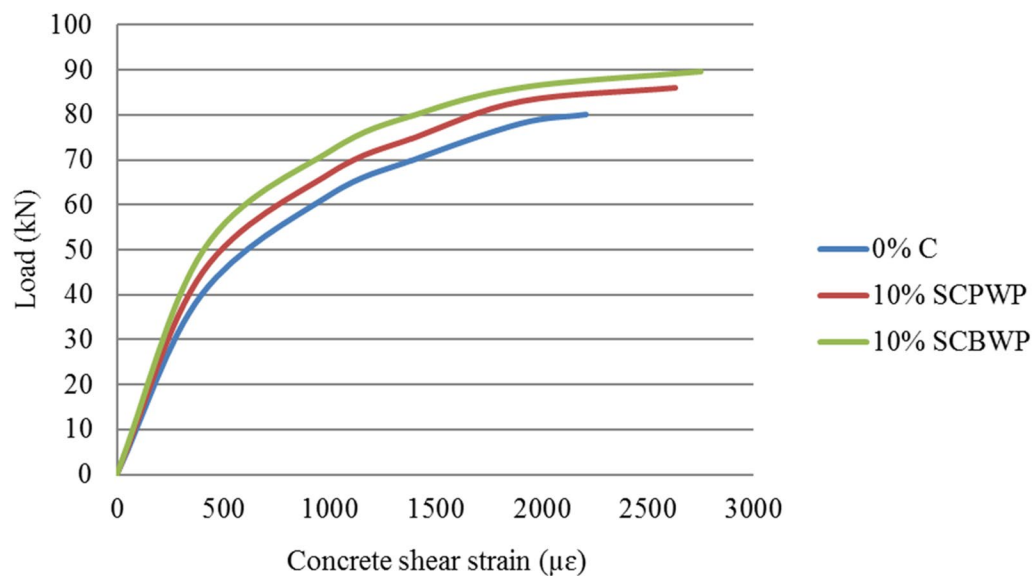


**Fig. 28** Load–strain (SS = 150 mm)

the ultimate concrete strength when the tensile load is increased (Jiang, 2003), which clarifies that the fibres were insufficient to avoid shear failure and rise the RCB shear strength. The failure of shear will be reduced if an adequate fibre amount is utilised in the RCB either with full or reduced shear reinforcement. RCB bottom fractures are increased and the width of the cracks are reduced by the fibre pullout mechanism, which works as a cracks arrester. Thus, the limited opening of diagonal cracks and increasing tension are influenced by fibre

inclusion in the RCB. Subsequently, the fibre controls the shear cracks and the aggregate interlock mechanism and improves the dowel movement of RCB (Martin, 2008).

In this study, the cracks initially propagate at the front and back surfaces of the RCB, followed by flexural failure with a further increase in load. Most of the cracks found were tiny, which decreased the crack numbers and width due to the fibre properties in the 10% SCPWP and 10% SCBWP concrete mixtures. It was proven that the structural behaviour of the RCB

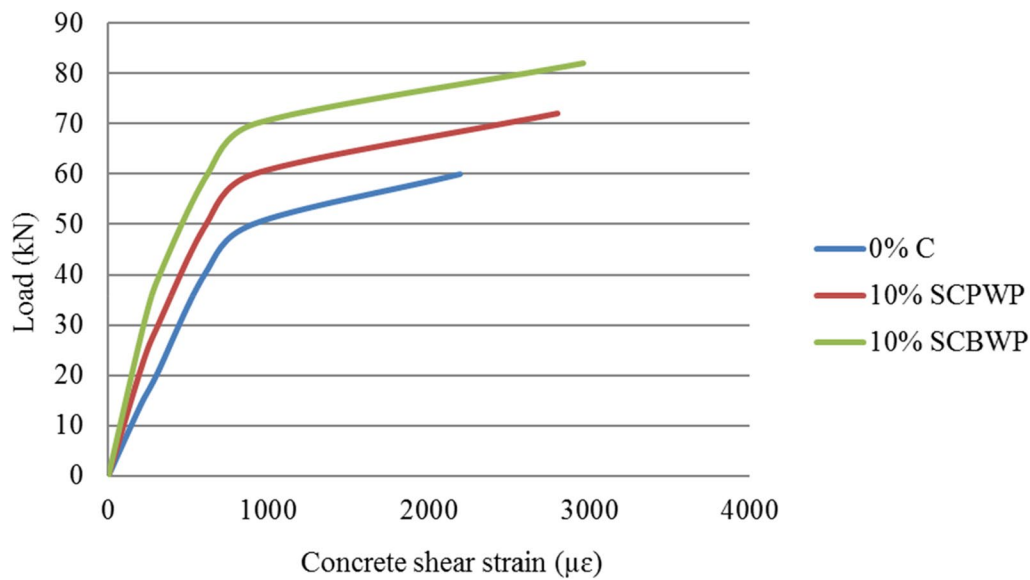


**Fig. 29** Load–strain (SS = 200 mm)

**Table 8** Load–strain

Stirrup spacing, SS (mm)	Concrete mixture	Concrete bending strain ( $\mu\epsilon$ )	Concrete shear strain ( $\mu\epsilon$ )
100	0% C	1900	2303
100	10% SCPWP	2053	2484
100	10% SCBWP	2127	2578
150	0% C	1805	2207
150	10% SCPWP	2228	2628
150	10% SCBWP	2347	2747
200	0% C	1784	2198
200	10% SCPWP	2450	2800
200	10% SCBWP	2572	2965

**Table 9** Ultimate and first crack loads

Stirrup spacing, SS (mm)	Concrete mixture	Load at first crack ( $P_1$ ) (kN)	Ultimate load ( $P_u$ ) (kN)
100	0% C	60.47	90.23
100	10% SCPWP	65.22	96.56
100	10% SCBWP	70.84	103.15
150	0% C	40.36	72.34
150	10% SCPWP	43.24	76.67
150	10% SCBWP	46.50	81.03
200	0% C	20.86	50.46
200	10% SCPWP	24.17	55.45
200	10% SCBWP	28.53	60.27

was improved throughout the pullout mechanism with fibre presence by preventing crack growth and increasing tensile properties (Solahuddin 2017; Solahuddin & Yahaya, 2021a, b, c, d, e, 2022; Solahuddin 2022a, b, c, d, e). Therefore, a sufficient fibre amount in 10% SCPWP and 10% SCBWP enhanced the shear reinforcement, changed shear strain to bending and failure mode, and prevented diagonal cracks. The results also show that the incorporation of fibre is compatibly utilised to control the RCB crack distribution and increases the load-carrying capacity after cracking. The RCB surface appeared to form more cracks as the load increases. In comparison, the 0% C failed because of the inadequate capacity of shear strength in the shear compression failure. Conversely, both 10% SCPWP and 10% SCBWP RCB show various behaviours of cracking with SS = 100 mm compared to other RCB with SS = 150 and 200 mm. The  $P_1$  detected the crack formations on the RCB surface near the middle span, and they were marked with a permanent red marker pen to show the crack formations. The flexural failure of the RCB caused the formation of vertical cracks on the RCB surface. Subsequently, the crack numbers increased with multiple cracking failures as the fibre amount increased. In conclusion, the formation of  $P_1$  is mainly affected by the amount of fibre from the SWP, which simultaneously increases the  $P_1$  load and reduces the crack width. Subsequently, it is found that a suitable fibre amount increases the RCB strengths, specifically,  $P_y$  and  $P_{max}$ .

**Table 10** Failure mode

Stirrup spacing (SS) (mm)	Concrete mixture	Failure mode	Failure location
100	0% C	Shear	A to B
100	10% SCPWP	Bending	B to C
100	10% SCBWP	Bending	B to C
150	0% C	Shear	A to B
150	10% SCPWP	Bending	B to C
150	10% SCBWP	Bending	B to C
200	0% C	Shear	A to B
200	10% SCPWP	Bending	B to C
200	10% SCBWP	Bending	B to C

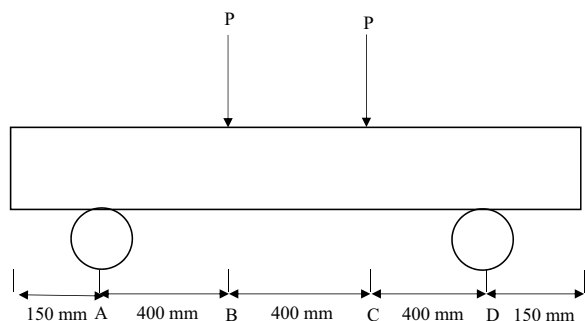


**Fig. 30** Key illustration of the RCB failure mode

**3.3.4 Failure Mode**

The results obtained for the failure mode of the RCB are summarised in Table 10. In addition to that, Fig. 30 shows the key illustration of the failure locations of the RCB.

Figs. 31, 32, and 33 show the cracking pattern and failure mode of SS=100 mm for 0% C, 10% SCPWP, and 10% SCBWP RCB, while for SS=150 mm for 0% C, 10% SCPWP, and 10% SCBWP RCB are shown in Figs. 34, 35, and 36, respectively. The first crack of 0% C for SS=100 mm and 150 mm occurs on the shear span located on the left (A to B). The load at first crack of the RCB increases with 10% SCPWP and 10% SCBWP addition compared to 0% C without 10% SCPWP and 10% SCBWP addition. These findings suggest that adding SWP to RCB, which has fibre content, delays the initiation of the first crack on the RCB surface. The crack lines of the (0% C, SS=100 mm) RCB appear in a constant moment region and penetrate vertically from the bottom to the top of the RCB (Fig. 31). In (0% C, SS=150 mm) RCB, the development of a diagonal crack on the left shear span appeared between the support and loading point, as shown in Fig. 34. Similar observations are shown in Figs. 32 and 35 for (SS=100 mm and 150 mm) RCB with 10% SCPWP, respectively. However, the crack propagation occurs at a flexural zone with crack initiation at the base, and the crack propagation continues towards the loading sites when the applied load



**Fig. 31** SS= 100 mm, 0% C



**Fig. 32** SS= 100 mm, 10% SCPWP



**Fig. 33** SS = 100 mm, 10% SCBWP



**Fig. 34** SS = 150 mm, 0% C



**Fig. 35** SS = 150 mm, 10% SCPWP



**Fig. 36** SS = 150 mm, 10% SCBWP

increases. For (SS = 100 mm, 10% SCBWP) RCB, the diagonal crack occurs on the mid-span and forms from the lower base towards the two upper loading points, as illustrated in Fig. 33. Furthermore, the crack propagation of (SS = 150 mm, 10% SCBWP) RCB appears at the bottom of the RCB surface and continues towards the RCB top on the left loading point, as depicted in Fig. 36.

Regarding the failure mode, if the RCB exhibits vertical cracks on the surface in a constant moment region,

it is commonly referred to as flexural cracks. The crack propagations outside a constant moment region are liked flexural cracks. However, if the cracks propagate outside the constant moment region and penetrate towards to support point, it is called shear cracks. This case may occur at higher loads with increasing shear stress. It can be observed that the RCB with SS = 100 mm with 0% C fails in shear, while 10% SCPWP and 10% SCBWP fail in bending. Besides that, in the situation of (SS = 150 mm,

0% C), it is observed to fail in shear. When SWP is added to the RCB, the failure mode changes from shear to bending, as shown by  $SS=150$  mm with both 10% SCPWP and 10% SCBWP concrete mixtures. Thus, the optimum amount addition of SCPWP and SCPWP, which is 10%, can improve the ductility, delay the crack propagation, and change the failure mode of the RCB from brittle to more ductile behaviour.

Figs. 37, 38, and 39 represent the cracking pattern of RCB for  $SS=200$  mm with 0% C, 10% SCPWP, and 10% SCBWP, respectively. The first crack load increases with the inclusion of 10% SCPWP and 10% SCBWP. These results confirm that adding SWP leads to a delay in crack propagation and creates multiple cracking that improves the RCB ductility. This study requires a high load to initiate the crack propagation. It can be clearly seen that most of the RCB shows cracking propagation along the mid-span and between the support point and loading. For  $SS=200$  mm with 10% SCPWP and 10% SCBWP, the crack propagations occur on the left shear span of the RCB and penetrate at an approximate distance of 400 mm away from the support towards the loading point (Figs. 38, 39). Based on the failure mode, it is observed that the RCB with  $SS=200$  mm with 10% SCPWP and

10% SCBWP fail in bending compared to 0% C due to a high dosage of fibre content that comes from the 10% SWP. It is noted that the RCB became stiffer at higher loads with less deflection and hence failed in bending mode. Additionally, as the SCPWP and SCBWP were added to the RCB, the failure mode altered from shear to bending. As a result, adding an optimum amount of SWP at 10% can improve the structural behaviour of RCB by improving the ductility, delaying crack propagation, and altering failure mode from brittle to more ductile behaviour.

#### 4 Conclusion

This study has demonstrated the potential use of SCPWP and SCBWP as additives to improve the properties of concrete and the structural behaviour of RCB. The test results revealed a clear understanding of the concrete's fresh, mechanical and durability properties with water curing conditions. Moreover, a significant structural behaviour of RCB is obtained through the addition of SCPWP and SCBWP. The following points conclude the findings of this study according to the research objectives:

- (i) Based on the slump data sets, the incorporation of SCPWP and SCBWP as additives at the percent-



**Fig. 37**  $SS=200$  mm, 0% C



**Fig. 38**  $SS=200$  mm, 10% SCPWP



**Fig. 39**  $SS=200$  mm, 10% SCBWP

ages of 5% and 10% addition increases the slump value. The addition of 10% SCBWP provides the highest slump value, while the utilisation of 15% SCPWP records the lowest slump value. Overall, SCBWP records higher slump values than SCPWP. Furthermore, the results indicate that the optimum SWP additions in the concrete mixture are 5% and 10%, while the inclusion of 15% SWP resulted in reducing workability. Hence, the SWP content significantly affects the workability of the concrete.

- (ii) The mechanical properties, such as compressive strength, flexural strength, and splitting tensile strength, under water curing regime increase from 7 and 28 days. The inclusion of 5% and 10% SCPWP and SCBWP in the concrete exhibits higher strengths, while the addition of 15% SCPWP and SCBWP produces the lowest concrete strength compared to the control concrete containing 0% of SWP. Apart from that, the utilisation of 10% SCPWP and SCBWP with water curing resulted in the highest compressive strength, flexural strength, and splitting tensile strength compared to other additional percentages. At 7 and 28 days, the highest compressive, flexural and splitting tensile strength values are recorded by 10% SCBWP addition, while the lowest strength values are exhibited by 15% of SCPWP addition. Generally, 5% and 10% addition of SCPWP and SCBWP are suitable additional percentages and 10% SCBWP addition as the optimum percentage. Therefore, it can be concluded that SCPWP and SCBWP are potentially used as additives material for new concrete production.
- (iii) The addition of 5% and 10% SCPWP and SCBWP enhances the concrete durability compared to the control concrete (0% SWP), to promote the lowest water absorption. Contrarily, 15% SCPWP and SCBWP records the highest water absorption as well as efflorescence. The higher percentages of SCPWP and SCBWP are prone to increase the water absorption values. Moreover, SCBWP shows a higher water absorption than SCPWP for all percentages. At 28 days, the highest water absorption value and efflorescence are recorded by 15% SCBWP addition, while the lowest water absorption value and efflorescence are recorded by 0% SWP addition.
- (iv) Compared to 0% C, the addition of 10% SCPWP and 10% SCBWP concrete mixtures, respectively, shows favourable contribution by improving the structural behaviour of RCB, including  $P_y$ ,  $P_u$ ,  $P_{max}$ ,  $P_1$ , and consequently decreasing  $\delta_y$ ,  $\delta_u$ , and  $\delta_{max}$  with full (SS=100 mm) and reduced shear

reinforcements (SS=150 mm, 200 mm), respectively. Moreover, the concrete bending and shear strains are also increased by the inclusion of 10% SCPWP and 10% SCBWP concrete mixtures for SS=100 mm, 150 mm, 200 mm. The 10% SCBWP RCB with SS=100 mm achieves the highest values of  $P_y$ ,  $P_u$ ,  $P_{max}$ , and  $P_1$  and the lowest values of  $\delta_y$ ,  $\delta_u$ , and  $\delta_{max}$ . It is found that 0% C with SS=200 mm records the lowest values of  $P_y$ ,  $P_u$ ,  $P_{max}$ , and  $P_1$  and the highest values of  $\delta_y$ ,  $\delta_u$ , and  $\delta_{max}$ . For concrete bending strain and concrete shear strain, the highest and lowest values are recorded by 10% SCBWP RCB and 0% RCB with SS=200 mm. The failure mode of the RCB also changes from shear to bending with the inclusion of 10% SCPWP and 10% SCBWP for all SS. Apparently, SCPWP and SCBWP with the optimum addition amount of 10% depict the best structural behaviour of RCB.

## 5 Recommendation

Generally, this study has demonstrated the potential use of SCPWP and SCBWP as additives in the production of concrete and RCB. The following recommendations are made based on the experimental results of this study:

- (i) This work needs to explore other WP types that might produce better concrete strengths.
- (ii) The addition of 5% and 10% of SCPWP and SCBWP was shown to accelerate the hydration process and enhance the strength. Thus, based on the mechanical properties, future research should focus on the effect of concrete after reacting with other percentages of SCPWP and SCBWP addition.
- (iii) The structural behaviour of RCB was improved with the fibre potential in 10% SCPWP and 10% SCBWP. Therefore, based on the fibre potential, it is recommended for further studies to evaluate the effect of RCB after reacting with other percentages of SCPWP and SCBWP addition.

### Acknowledgements

The authors would like to acknowledge Universiti Malaysia Pahang (UMP), Malaysia, for financially supporting this research through UMP Postgraduate Research Grant Scheme (PGRS200373).

### Author contributions

BAS contributed to conceptualisation, resources, data curation, writing—original draft preparation, and writing—review and editing; BAS and FMY performed investigation. All the authors have read and agreed to the published version of this manuscript.

### Authors' information

B. A. Solahuddin, M.Sc student; F. M. Yahaya, Senior lecturer and Faculty of Civil Engineering Technology, Universiti Malaysia Pahang, Lebuhraya Tun Razak, 26300 Gambang, Kuantan, Pahang Darul Makmur, Malaysia.

**Funding**

The authors would like to acknowledge Universiti Malaysia Pahang (UMP), Malaysia, for financially supporting this research through UMP Postgraduate Research Grant Scheme (PGRS200373).

**Availability of data and materials**

Data sharing not applicable: no new data were created or analysed in this study. Data sharing is not applicable to this article.

**Declarations****Ethics approval and consent to participate**

Not applicable.

**Consent for publication**

Not applicable.

**Competing interests**

The authors declare no competing interests.

Received: 27 December 2022 Accepted: 4 February 2023

Published online: 24 April 2023

**References**

- Akinwande, A. A., Adediran, A. A., Balogun, O. A., Adesina, O. S., Olasoju, O. S., Owa, A. F., Erinle, T. J., & Akinlabi, E. T. (2021a). Assessment of alkaline treatment of palm kernel fiber and curing duration on selected properties of cement-paper composite boards. *Cogent Engineering*, 8(1). <https://doi.org/10.1080/23311916.2021.1909690>.
- Akinwande, A. A., Adediran, A. A., Balogun, O. A., Olusoj, O. S., & Adesina, O. S. (2021b). Influence of alkaline modification on selected properties of banana fiber paperbricks. *Scientific Reports*, 11(1), 1–18. <https://doi.org/10.1038/s41598-021-85106-8>
- Akinwande, A. A., Balogun, O. A., Romanovski, V., Danso, H., Ademati, A. O., & Adetula, Y. V. (2022). Recycling of synthetic waste wig fiber in the production of cement-adobe for building envelope: physio-hydric properties. *Environmental Science and Pollution Research*, 29, 34075–34091. <https://doi.org/10.1007/s11356-022-18649-6>
- Akinwumi, I. I., & Gbadamosi, Z. O. (2014). Effects of curing condition and curing period on the compressive strength development of plain concrete. *International Journal of Civil and Environmental Research*, 1(2), 83–99.
- ASTM C1609/C1609M19, Standard test method for flexural performance of fiber-reinforced concrete using beam with four-point loading.
- Bai, J., Chaipanich, A., Kinuthia, J. M., O'Farrell, M., Sabir, B. B., Wild, S., & Lewis, M. H. (2003). Compressive strength and hydration of wastepaper sludge ash-ground granulated blastfurnace slag blended pastes. *Cement and Concrete Research*, 33(8), 1189–1202. [https://doi.org/10.1016/S0008-8846\(03\)00042-5](https://doi.org/10.1016/S0008-8846(03)00042-5)
- Balwaik, S. A., & Raut, S. P. (2011). Utilization of waste paper pulp by partial replacement of cement in concrete. *International Journal of Engineering Research and Applications*, 1(2), 300–309.
- Beskopylny, A. N., Shcherban, E. M., Stelmakh, S. A., Meskhi, B., Shilov, A. A., Varavka, V., Evtushenko, A., Özkılıç, Y. O., Aksoylu, C., & Karalar, M. (2022). Composition component influence on concrete properties with the additive of rubber tree seed shells. *Applied Sciences (Switzerland)*, 12(22). <https://doi.org/10.3390/app122211744>
- Borysiuk, P., Nicewicz, D., Pawlicki, J., & Klimczewski, M. (2017). The influence of the type and preparation of ligno-cellulose fibres on the properties of MDF. *Wood Research*, 52(4), 79–88.
- British Standard Institution. (1983). Testing concrete. Method for making test cubes from fresh concrete. London, BS 1881: Part 108.
- British Standards Institution. (1985). Specification for Aggregates from natural sources for concrete minimum and maximum cumulative percentage passing: BS 812.
- British Standards Institution. (1992). Specification for Aggregates from natural sources for concrete: BS 882.
- British Standard Institution. (2013). Testing concrete. Methods for mixing and sampling fresh concrete in the laboratory. London, BS 1881: Part 125.
- Cardinale, T., D'amato, M., Sulla, R., & Cardinale, N. (2021). Mechanical and physical characterization of papercrete as new eco-friendly construction material. *Applied Sciences (Switzerland)*, 11(3), 1–11. <https://doi.org/10.3390/app11031011>
- Çelik, A. İ., Özkılıç, Y. O., Zeybek, Ö., Karalar, M., Qaidi, S., Ahmad, J., Burduhos-Nergis, D. D., & Bejinariu, C. (2022b). Mechanical behavior of crushed waste glass as replacement of aggregates. *Materials*, 15(22). <https://doi.org/10.3390/ma15228093>.
- Çelik, A. İ., Özkılıç, Y. O., Zeybek, Ö., Özdöner, N., & Tayeh, B. A. (2022a). Performance assessment of fiber-reinforced concrete produced with waste lathe fibers. *Sustainability (Switzerland)*, 14(19). <https://doi.org/10.3390/su141911817>.
- Chin, T. L., et al. (1998). A novel method to reuse paper sludge and co-generation ashes from paper mill. *Journal of Hazardous Materials*, 58(1–3), 93–102.
- Chun, Y., Naik, T., & Kraus, R. (2007). Pulp and paper mill fibrous residuals in excavatable flowable fill. In *Presented at the International Conference on Sustainable Construction Materials and Technologies*.
- Civil E Blog, 2020. <https://civileblog.com/concrete-mix-ratio/>
- Construction Cost, 2021. <https://www.constructioncost.co/concrete-mix-ratio.html>
- Emmanuel Ofori, 2019. [https://www.academia.edu/38360343/CONCRETE\\_GRADES\\_WITH\\_THEIR\\_RESPECTIVE\\_MIX\\_RATIOS](https://www.academia.edu/38360343/CONCRETE_GRADES_WITH_THEIR_RESPECTIVE_MIX_RATIOS)
- Fuwape, J. A., Fabyi, J. S., & Osuntuyi, E. O. (2007). Technical assessment of three layered cement-bonded boards produced from wastepaper and sawdust. *Waste Management*, 27(11), 1611–1616. <https://doi.org/10.1016/j.wasman.2006.09.005>
- Gallardo, R. S., & Adajar, M. A. Q. (2006). Structural performance of concrete with paper sludge as fine aggregates partial. In *International Symposium on Environmental Engineering and 5th Regional Symposium on Infrastructure Development, May*, 1–8.
- Ghani, A. N. A., & Mohammad Shukeri, R. (2008). Concrete mix with wastepaper. In *2nd International Conference on Built Environment in Developing Countries (ICBEDC), Penang, Malaysia, University Sains Malaysia (USM), Icbdec*, 567–575. <http://eprints.usm.my/34459/1/HBP15.pdf>.
- Hospodarova, V., Stevulova, N., Briancin, J., & Kostelanska, K. (2018). Investigation of waste paper cellulosic fibers utilization into cement based building materials. *Buildings*, 8(3), 10–12. <https://doi.org/10.3390/buildings8030043>
- Jiang, P. H. (2003). Tension stiffening and cracking of steel fiber-reinforced concrete. *Journal of Materials in Civil Engineering*, 15(2), 174–182.
- Jung, H. S., Choi, H. K., & Choi, C. S. (2015). An experimental study on development of construction concrete products using wastepaper. *Journal of Ceramic Processing Research*, 16, 104–109.
- Kalapad, J. D., Mansute, M., Swami, V., Sulbhewar, V., & Khandale, T. M. (2019). A study on partial replacement of cement by waste paper pulp in concrete. *International Journal of Innovations in Engineering and Science*, 4(4), 2456–3463.
- Karalar, M., Bilir, T., Çavuşlu, M., Özkılıç, Y. O., & Sabri Sabri, M. M. (2022b). Use of recycled coal bottom ash in reinforced concrete beams as replacement for aggregate. *Frontiers in Materials*, 9, 1–19. <https://doi.org/10.3389/fmats.2022.1064604>
- Karalar, M., Özkılıç, Y. O., Aksoylu, C., Sabri Sabri, M. M., Beskopylny, A. N., Stelmakh, S. A., & Shcherban, E. M. (2022c). Flexural behavior of reinforced concrete beams using waste marble powder towards application of sustainable concrete. *Frontiers in Materials*, 9(December), 1–14. <https://doi.org/10.3389/fmats.2022.1068791>
- Karalar, M., Özkılıç, Y. O., Deifalla, A. F., Aksoylu, C., Arslan, M. H., Ahmad, M., & Sabri, M. M. S. (2022a). Improvement in bending performance of reinforced concrete beams produced with waste lathe scraps. *Sustainability (Switzerland)*, 14(19), 1–17. <https://doi.org/10.3390/su141912660>
- Khan Academy. (2016). <https://www.khanacademy.org/humanities/ap-art-history/late-europe-and-americas/modernity-ap/a/frank-lloyd-wright-fallingwater>.
- Khan, A. S., & Zhang, H. (2000). Mechanically alloyed nanocrystalline iron and copper mixture: Behavior and constitutive modeling over a wide range of strain rates. *International Journal of Plasticity*, 16(12), 1477–1492.

- Kraus, R. N., et al. (2003). Concrete containing recycled fibers from pulp and paper mills. In *Sixth CANMET/ACI International Conference June 2003, Recent Advances in Concrete Technology*. Bucharest, Romania.
- Li, A. E., Alkhairi, F. M., & Hammoud, H. (2013). Fiber reinforced concrete. *ACI Journal*, 59, 351–374.
- Malik, M. I. (2013). Study of concrete involving use of waste glass as partial replacement of fine aggregates. *IOSR Journal of Engineering*, 3(7), 08–13. <https://doi.org/10.9790/3021-03760813>
- Malthy, R., & Jegatheeswaran, D. (2011). Comparative study on concrete bricks with conventional bricks. *ICI Journal*.
- Martin, A. M. (2008). Fibre reinforced cement-based (FRC) composites after over 40 years of development in building and civil engineering. *Composite Structures*, 86(1), 3–9.
- MS 522: Part 1: 2003, Ms 522 Part 12003 Portland Cement (Ordinary and Rapid-Hardening) Part 1 Specification (Second Revision)-709539.
- Naik, T. R., Friberg, T. S., & Chun, Y. M. (2004). Use of pulp and paper mill residual solids in production of cellucrete. *Cement and Concrete Research*, 34(7), 1229–1234. <https://doi.org/10.1016/j.cemconres.2003.12.013>
- Neville, A. M. (2011). *Properties of concrete* (5th ed.). Longman, Malaysia.
- Okino, E. Y. A., Santana, M. A. E., & De Souza, M. R. (2000). Utilisation of waste-paper to manufacture low density boards. *Bioresource Technology*, 73(1), 77–79. [https://doi.org/10.1016/S0960-8524\(99\)00146-7](https://doi.org/10.1016/S0960-8524(99)00146-7)
- Özkılıç, Y. O., Zeybek, Ö., Çelik, A. İ., Deifalla, A., Ahmad, M., & Sabri, M. (2022). Performance evaluation of fiber-reinforced concretes produced with steel fibers extracted from waste tire. *Frontiers in Materials*, 692. <https://doi.org/10.3389/fmats.2022.1057128>.
- Prasad, G. V. S., Reddy, P. P., Swathi, M., Kumar, P. D. V., Praveenraja T., Naveen M., 2015. In *J of Eng R*. 3. 3.
- Qaidi, S., Najm, H. M., Abed, S. M., Özkılıç, Y. O., Al Dughaisi, H., Alost, M., Sabri, M. M. S., Alkhatib, F., & Milad, A. (2022). Concrete containing waste glass as an environmentally friendly aggregate: a review on fresh and mechanical characteristics. *Materials*, 15(18), 1–16. <https://doi.org/10.3390/ma15186222>
- Sangrutsamee, V., Srichandr, P., & Poolthong, N. (2012). Re-pulped waste paper-based composite building materials with low thermal conductivity. *Journal of Asian Architecture and Building Engineering*, 11(1), 147–151. <https://doi.org/10.3130/jaabe.11.147>
- Science Buddies (2015). Folded or flat paper towel: which one absorbs more water? Bring Science Home.
- Shcherban, E. M., Stelmakh, S. A., Beskopylny, A. N., Mailyan, L. R., Meskhi, B., Shilov, A. A., Chernilnik, A., Özkılıç, Y. O., & Aksoyly, C. (2022). Normal-weight concrete with improved stress–strain characteristics reinforced with dispersed coconut fibers. *Applied Sciences (Switzerland)*, 12(22). <https://doi.org/10.3390/app122211734>.
- Sin, L. H., Huan, W. T., Islam, M. R., & Mansur, M. A. (2011). Reinforced lightweight concrete beams in flexure. *ACI Structural Journal*, 108(1), 3–12.
- Solahuddin B. A. (2017). *The Effect of Shredded Paper as Partial Sand Replacement on Properties of Cement Sand Brick*. Bachelor's Degree Thesis, Universiti Malaysia Pahang.
- Solahuddin, B. A. (2022a). A critical review on experimental investigation and finite element analysis on structural performance of kenaf fibre reinforced concrete. *Structures*, 35, 1030–1061. <https://doi.org/10.1016/j.istruc.2021.11.056>
- Solahuddin, B. A. (2022b). A review on structural performance of bamboo reinforced concrete. *Materials Science Forum*, 1056 MSF, 75–80. <https://doi.org/10.4028/p-dx1x87>.
- Solahuddin, B. A. (2022c). Strengthening of reinforced concrete with steel fibre: a review. *Materials Science Forum*, 1056(2017), 81–86. <https://doi.org/10.4028/p-3g0h57>
- Solahuddin, B. A. (2022d). A review on the effect of reinforcement on reinforced concrete beam-column joint behavior. *Proceedings of Malaysian Technical Universities Conference on Engineering and Technology (MUCET) 2021*.
- Solahuddin, B. A. (2022e). Seismic Performance of Reinforced Concrete Beam-Column Joint: A Review. *Proceedings of Malaysian Technical Universities Conference on Engineering and Technology (MUCET) 2021*.
- Solahuddin, B. A. (2022f). A comprehensive review on waste paper concrete. *Results in Engineering*, 16, 100740. <https://doi.org/10.1016/j.rineng.2022.100740>
- Solahuddin, B. A., & Yahaya, F. M. (2021a). Effect of shredded waste paper on properties of concrete. *IOP Conference Series: Materials Science and Engineering*, 1092(1), 012063. <https://doi.org/10.1088/1757-899x/1092/1/012063>
- Solahuddin, B. A., & Yahaya, F. M. (2021b). Load-strain behaviour of shredded waste paper reinforced concrete beam. *IOP Conference Series: Materials Science and Engineering*, 1092(1), 012063. <https://doi.org/10.1088/1757-899x/1092/1/012063>
- Solahuddin, B. A., & Yahaya, F. M. (2021c). A review paper on the effect of waste paper on mechanical properties of concrete. *IOP Conference Series: Materials Science and Engineering*, 1092(1), 012063. <https://doi.org/10.1088/1757-899x/1092/1/012067>
- Solahuddin, B. A., & Yahaya, F. M. (2021d). Structural behaviour of shredded waste paper reinforced concrete beam. *International Journal of Advanced Research in Engineering Innovation*, 3(1), 74–87.
- Solahuddin, B. A., & Yahaya, F. M. (2021e). Inclusion of waste paper on concrete properties: a review. *Civil Engineering Journal Tehran*, 7(94), 94–113. <https://doi.org/10.28991/CEJ-SP2021-07-07>
- Solahuddin, B. A., & Yahaya, F. M. (2022). Properties of concrete containing shredded waste paper as an additive. *Materials Today Proceedings*, 51, 1350–1354. <https://doi.org/10.1016/j.matpr.2021.11.390>
- Syed Mohsin, S.M. (2012). Behaviour of fibre-reinforced concrete structures under seismic loading. Ph.D thesis, Imperial College London, UK.
- Thiswaran, Y. D. (2018). Paper Crete : A lightweight concrete Concrete : A Lightweight Concrete.
- Thiswaran, M. Y. D., & Varma, D. M. B. (2017). Properties of concrete crete: building material. *IOSR Journal of Mechanical and Civil Engineering*, 14(02), 27–32. <https://doi.org/10.9790/1684-1402072732>
- Titzman, L. C. (2006). Analysis of low-cost building material for the mixalco process analysis of low-cost building material for the Mixalco process. Uniform Building Code, 2017. [https://en.wikipedia.org/wiki/Uniform\\_Building\\_Code](https://en.wikipedia.org/wiki/Uniform_Building_Code)
- Wagih, A. M., El-Karmoty, H. Z., Ebid, M., & Okba, S. H. (2013). Recycled construction and demolition concrete waste as aggregate for structural concrete. *HBRC Journal*, 9(3), 193–200. <https://doi.org/10.1016/j.hbrj.2013.08.007>
- Yun, H., Jung, H., & Choi, C. (2011). Mechanical properties of concrete containing waste paper. *ICCM International Conferences on Composite Materials*, 1–4.
- Zaki, H., Gorgis, I., & Salih, S. (2018). Mechanical properties of concrete. *MATEC Web of Conferences*, 162(January). <https://doi.org/10.1051/mateconf/201816202016>.
- Zeybek, Ö., Özkılıç, Y. O., Karalar, M., Çelik, A. İ., Qaidi, S., Ahmad, J., Burduhos-Nergis, D. D., & Burduhos-Nergis, D. P. (2022). Influence of replacing cement with waste glass on mechanical properties of concrete. *Materials*, 15(21), 7513. <https://doi.org/10.3390/ma15217513>

## Publisher's Note

Springer Nature remains neutral with regard to jurisdictional claims in published maps and institutional affiliations.

**Submit your manuscript to a SpringerOpen® journal and benefit from:**

- Convenient online submission
- Rigorous peer review
- Open access: articles freely available online
- High visibility within the field
- Retaining the copyright to your article

Submit your next manuscript at ► [springeropen.com](https://www.springeropen.com)